Selective Fluorescent Nonpeptidic Antagonists For Vasopressin V-2 GPCR: Application To Ligand Screening and Oligomerization Assays

ARTICLE *in* JOURNAL OF MEDICINAL CHEMISTRY · SEPTEMBER 2012

Impact Factor: 5.45 · DOI: 10.1021/jm3006146 · Source: PubMed

Journal of Medicinal Chemistry

Article

pubs.acs.org/jmc

Selective Fluorescent Nonpeptidic Antagonists For Vasopressin V_2 GPCR: Application To Ligand Screening and Oligomerization Assays.

Stéphanie Loison,[†] Martin Cottet,[‡] Hélène Orcel,[‡] Hélène Adihou,[†] Rita Rahmeh,[‡] Laurent Lamarque,[§] Eric Trinquet,[§] Esther Kellenberger,[†] Marcel Hibert,[†] Thierry Durroux,[‡] Bernard Mouillac,[‡] and Dominique Bonnet*[,†]

[†]Laboratoire d'Innovation Thérapeutique, UMR7200 CNRS/Université de Strasbourg, Faculté de Pharmacie, 74 route du Rhin, 67412 Illkirch, France

[‡]CNRS UMR 5203, INSERM U661, and Université Montpellier I et II, Institut de Génomique Fonctionnelle, Département de Pharmacologie Moléculaire, 141 rue de la Cardonille, 34094 Montpellier Cedex 5, France

[§]Cisbio Bioassays, Parc Marcel Boiteux, BP84175, 30200 Codolet, France

Supporting Information

ABSTRACT: A series of fluorescent benzazepine ligands for the arginine−vasopressin V_2 receptor (AVP V_2R) was synthesized using "Click" chemistry. Their in vitro pharmacological profile at AVP V_2R, $V_{1a}R$, $V_{1b}R$, and oxytocin receptor was measured by binding assay and functional studies. Compound **9p**, labeled with Lissamine Rhodamine B using novel solid-phase organic tagging (SPOrT) resin, exhibited a high affinity for V_2R (4.0 nM), an excellent selectivity toward V_2R and antagonist properties. By changing the nature of the dye, DY647 and Lumi4-Tb probes **44** and **47** still display a high affinity for V_2R (5.6 and 5.8 nM, respectively). These antagonists constitute the first high-affinity selective nonpeptidic fluorescent ligands for V_2R. They enabled the development of V_2R time-resolved FRET-based assay readily amenable to high-throughput screening. Taking advantage of their selectivity, these compounds were also successfully involved in the study of $V_{1a}R$−V_2R dimerization on cell surface.

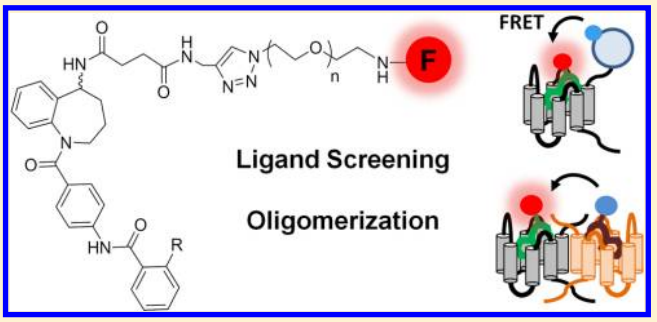

INTRODUCTION

G protein-coupled receptors (GPCRs) constitute the largest family of transmembrane signaling molecules in the human genome and represent the most important class of therapeutic targets to the pharmaceutical industry.[1−3] It is of importance to gain a better understanding of their functioning and their molecular structure but also to set up new receptor-selective high-throughput screening (HTS) assays. Owing to their high sensitivity and to their reduced environmental safety risk, fluorescent technologies represent a powerful molecular tool to perform these studies.[4] Fluorescence polarization constitutes a very useful and convenient method for binding studies and can be readily amenable to HTS for drug discovery.[5−7] Fluorescence resonance energy transfer (FRET) between a fluorescent donor−acceptor pair has also been shown to be a convenient method to investigate intra- and intermolecular interaction processes both in vitro and in vivo.[8−10] Time-resolved fluorescence resonance energy transfer (TR-FRET), utilizing rare-earth lanthanides with long emission half-lives as donor fluorophores, combines standard FRET with the time-resolved measurement of fluorescence. This powerful combination provides significant benefits for HTS[11,12] and also for the study of GPCRs oligomerization both at the surface of living cells[13] and more recently in native tissues.[14] Nevertheless, the prerequisite for the development of such fluorometric assays is to design, to synthesize, and to characterize fluorescent ligands that retain the pharmacological profile of the nonlabeled probes. Ideally, fluorescent probes should be nonpeptidic to improve their in vivo metabolic stability and should display high affinity but also selectivity for a given receptor subtype. Unlike fluorescent peptides, the design of fluorescent small-molecule ligands for GPCRs is not trivial.[15] Indeed, the potential site for fluorophore conjugation is usually in much closer proximity to the pharmacophore and, as a consequence, is much more likely to compromise ligand affinity and efficacy.[8]

Arginine−vasopressin (AVP) V_2 receptor (V_2R) is a GPCR that continues to generate significant interest in drug discovery as highlighted by the recent development of nonpeptidic V_2R antagonists, namely Conivaptan (Astellas) and Tolvaptan (Otsuka), approved by the FDA for the treatment of hyponatremia.[16] In addition, vasopressin V_2R is also considered as a drug target for the potential treatment of various diseases such as congestive heart failure, hypertension, edema, or several renal pathologies such as congenital nephrogenic diabetes insipidus.[17,18] To accelerate the discovery of new ligands for

Received: May 3, 2012

   dx.doi.org/10.1021/jm3006146 | J. Med. Chem. XXXX, XXX, XXX−XXX

V_2R, we decided to setup a FRET-based assay with the prerequisite to develop selective fluorescent ligands. Although various peptidic or nonpeptidic agonists and antagonists for V_2R have been described in the literature,[19] only very few fluorescent ligands for this GPCR have been reported.[20,21] In addition, these fluorescent probes are peptidic and nonselective for V_2R with respect to V_{1a}, V_{1b}, and oxytocin receptors (OTR). No selective fluorescent nonpeptidic ligand for V_2R has been reported to date.

In this article, we describe the first high affinity and selective fluorescent nonpeptidic antagonists for V_2R, derived from the 2,3,4,5-tetrahydro-1*H*-benzo[*b*]azepine scaffold. The synthesis were performed either on solid-phase by using our recent solid-phase organic tagging (SPOrT) resin[22] or in solution, enabling the convenient incorporation of different dyes through various spacers. The influence of the nature and the length of the spacers on both the affinity and the selectivity of the fluorescent probes toward V_2R were carefully evaluated. The most potent ligands were found useful tools for developing new V_2R-selective HTS assays and for investigating V_2R–$V_{1a}R$ dimerization at the surface of living cell by TR-FRET.

RESULTS AND DISCUSSION

Design of Fluorophore-Tagged Vasopressin GPCR Ligands. Our approach was to prepare fluorescent probes for V_2R by linking fluorescent tags to nonpeptide V_2R antagonists **1** and **2** through various spacers (Figure 1).

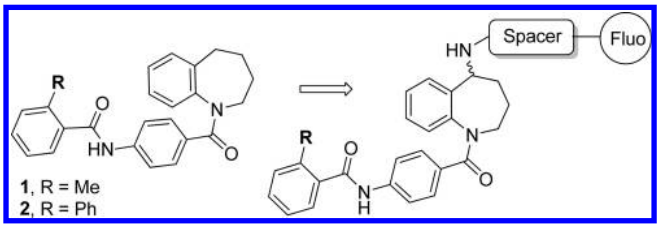

Figure 1. General strategy for the labeling of 2,3,4,5-tetrahydro-1*H*-benzo[*b*]azepines derivatives.

Compound **1** (*o*-toluoyl derivative) has been described as nonselective high-affinity antagonist for AVP $V_{1a}R$, V_2R, and OTR (Figure 2).[23] The structure–activity relationships have shown that the introduction of a basic group, such as a dimethylamine, at the 5-position of the benzazepine ring (OPC-31260, Figure 2) have little effect on the binding affinity for V_2R but leads to a reduction of the $V_{1a}R$ and OTR binding affinities. On the other hand, the introduction of an aromatic

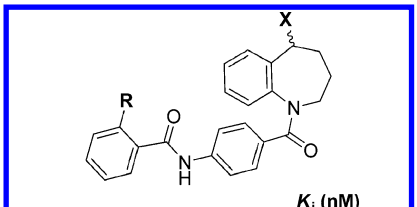

Cpd	X	R	K_i (nM) V2	V1a	OT
1	-H	-Me	7.2	8.1	30
OPC-31260	$-NMe_2$	-Me	9.7	195	660
2	-H	-Ph	7.5	14.1	63

Figure 2. Reported binding affinities of compounds **1**, **2**, and OPC-31260 for V_2R, $V_{1a}R$, and OTR.[23,24]

ring in place of a methyl group on the benzoyl moiety (compound **2**, Figure 2) has been reported to enhance the antagonist activity of the compound for V_2R but neither its affinity nor its selectivity.[24] On the basis of these results, the attachment of the dye to compounds **1** and **2** was envisaged at the 5-position of the benzazepine scaffold through various spacers of different chemical nature and length. With the aim to improve the general solubility of the fluorescent probes, spacers containing pegylated[25,26] or piperazine[27] moieties were synthesized. To conduct the studies, the LRB dye was first selected due to its large molar extinction coefficient (88000 $cm^{-1}\cdot M^{-1}$) combined with an excellent chemical and photostability. Additionally, it is readily accessible from commercial sources in amounts compatible with synthetic organic chemistry. This dye has found applications for molecular imaging both in vitro[28] and in vivo.[29] In addition, LRB has been described in our group as an energy acceptor from excited EGFP to study ligand–GPCR interactions by FRET.[8,30] Fluorescein and DY647 (Dyomics) exhibit well suited spectroscopic properties for TR-FRET approaches. Lumi4-Tb (Lumiphore Inc.), a lanthanide complexe,[31] has been developed because of its long fluorescent lifetime which allows specific signal to be time-resolved from nonspecific signal.[32]

Synthesis, Solubility, and Spectroscopic Characterization of Lissamine Rhodamine B (LRB) Probes. The synthesis of the fluorescent LRB-labeled benzazepine derivatives was first undertaken on solid-phase starting from our novel SPOrT resin.[22] This resin has been developed to facilitate the labeling of both peptides and small organic compounds via a Cu(I) catalyzed 1,3-cycloaddition, referred to as "Click" chemistry. As previously described for *o*-toluoyl fluorescent probes **8o,p**,[22] biphenyl derivatives **9o,p** were readily obtained in seven steps (Scheme 1). Briefly, 2,3,4,5-tetrahydro-1*H*-benzo[*b*]azepin-5-amino scaffold[33] was loaded on the resin by using PyBOP in situ activation.[34] Following Boc deprotection in the presence of trimethylsilyl trifluoromethanesulfonate (TMSOTf) and Et_3N,[35] the endocyclic nitrogen was reacted with 4-nitrobenzoyl chloride in the presence of pyridine and 4-dimethylpyridine (4-DMAP) to access resin **3**, which was subsequently treated with $SnCl_2$ to perform the nitro group reduction (resin **4**). The resulting aniline derivative was acylated with 2-methylbenzoyl chloride or 2-biphenylcarbonyl chloride to display resin **5** and **6**, respectively. Both resins were then submitted to a Cu(I)-catalyzed 1,3-dipolar cycloaddition in the presence of Lissamine-$(PEG)_3$-azido **7** (mixture of ortho and para isomers). Treatment in acidic conditions of the resin-bound LRB benzazepines enables the access to compounds **8** and **9** obtained as a mixture of ortho **8o** and **9o** and para **8p** and **9p** isomers (Scheme 1). Their separation was achieved by reverse-phase high-performance liquid chromatography (RP-HPLC), the major para isomer displaying a higher retention time than the ortho derivative. The two regioisomers were unambiguously characterized by ^1H NMR. Indeed, in agreement with previous reports on the identification of LRB isomers,[22,36] the H5 proton of the lissamine moiety (Scheme 1) in the ortho-isomer was found downfield to the corresponding one in the para-isomer.

To evaluate the influence of the chemical nature and the length of the spacers onto the solubility and on the pharmacological profile of the ligands, a solution-phase approach was also developed (Scheme 2). The key step was the coupling of the amino-benzazepine scaffold **10** either directly with LRB dye or through various spacers incorporating

dx.doi.org/10.1021/jm3006146 | J. Med. Chem. XXXX, XXX, XXX–XXX

Scheme 1. Solid-Phase Synthesis of Lissamine Labeled Benzazepines Using "SPOrT" Resin[a]

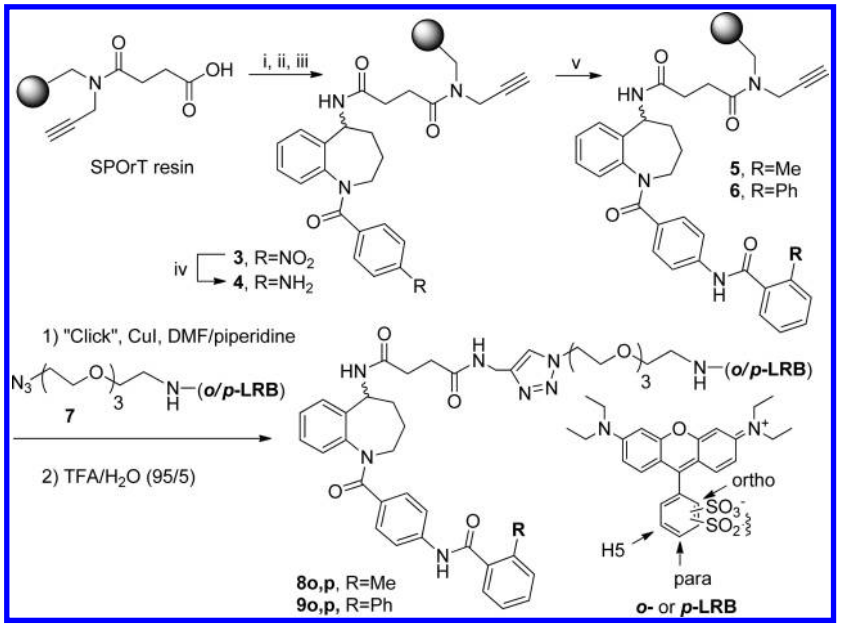

[a]Reagents: (i) 2,3,4,5-tetrahydro-1*H*-benzo[*b*]azepin-5-amino scaffold, PyBOP, Hünig's base, DMF; (ii) TMSOTf, Et_3N, CH_2Cl_2; (iii) *p*-NO_2BzCl, pyridine, 4-DMAP, CH_2Cl_2; (iv) $SnCl_2$, $2H_2O$, DMF; (v) 2-methylbenzoyl chloride or 2-biphenylcarbonyl chloride, Hünig's base, 4-DMAP, CH_2Cl_2.

Scheme 2. Synthesis of Various *para*-Lissamine Rhodamine B (*p*-LRB) Derived Spacers for the Functionalization of Benzazepines 1 and 2[a]

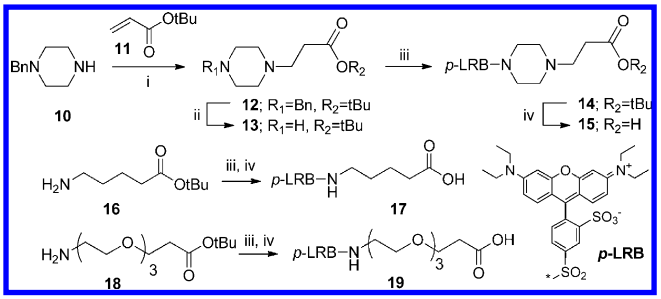

[a]Reagents: (i) $CHCl_3$/MeOH; (ii) Pd/C, H_2, MeOH; (iii) *p*-LRB sulfonyl chloride, Hünig's base, CH_2Cl_2; (iv) TFA/CH_2Cl_2/H_2O.

an alkyl chain or a more soluble piperazine or PEG moieties. To avoid the tedious final separation of *ortho*- and *para*-LRB isomers, we envisaged the regioselective activation of LRB sulfonyl chlroride by treating commercially available Acid Red 52 sodium salt with oxalyl chloride in the presence of catalytic amount of DMF.[37]

Piperazine spacer **15** was obtained in a four-step process starting from 1-Boc-piperazine **10**. 1,4-Michael addition of an excess of **10** on acrylate **11** in a $CHCl_3$/MeOH mixture led to benzyl ester **12** in 94% yield. The subsequent hydrogenolysis of benzyl protecting group was followed by the sulfonylation of piperazine **13** with *p*-LRB sulfonyl chloride. Piperazine spacer **14** was thus obtained as a single para-isomer in 47% yield. The final *t*Bu ester hydrolysis in the presence of TFA enabled the clean access to acid **15** in 42% overall yield (four steps). Alkylated and pegylated spacers **17** and **18** were readily obtained in two steps (sulfonylation and deprotection) from commercially available ester **16** and **18** in 38% and 54% overall yields, respectively (Scheme 2).

p-LRB spacers were incorporated onto the amino-benzazepine **26** that was obtained in a five-step process starting from commercially available methyl 4-aminobenzoate **20** (Scheme 3). The acylation of **20** with the acyl chloride of 2-biphenyl

Scheme 3. Solution-Phase Synthesis of *p*-LRB Labeled Benzazepines 27−30[a]

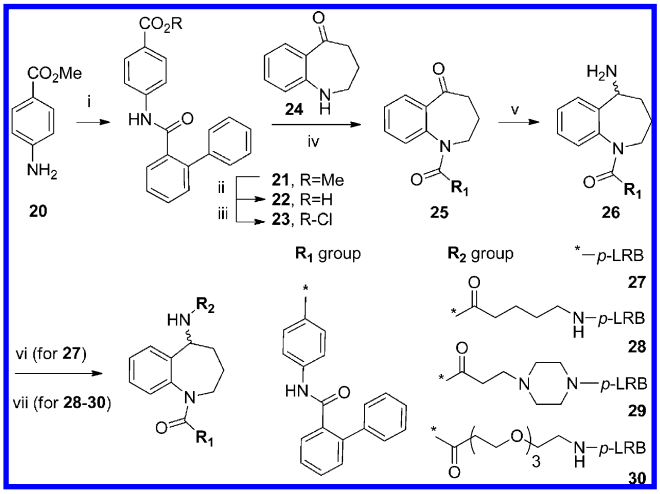

[a]Reagents: (i) (a) 2-biphenyl carboxylic acid, $SOCl_2$, NMP, CH_2Cl_2, (b) Hünig's base, CH_2Cl_2; (ii) HCl 6 N/AcOH (1/1); (iii) $SOCl_2$, NMP, CH_2Cl_2; (iv) pyridine, 4-DMAP, CH_2Cl_2; (v) NH_4OAc, $NaBH_3CN$, MeOH, μW, 100 °C, 2 × 5 min; (vi) *para*-Lissamine Rhodamine B sulfonyl chloride, Hünig's base, DMAP, CH_2Cl_2, DMF; (vii) spacers **15**, **17**, and **19**, PyBOP, Hünig's base, DMF.

carboxylic acid gave ester **13** that was hydrolyzed in acidic conditions to the corresponding acid **22** (82% yield, 2 steps). Its subsequent coupling with benzazepinone scaffold **24** using various activating agents such as PyBOP and HBTU/HATU failed to furnish the expected compound **25**. The best result was obtained by using the corresponding acyl chloride **23**,

dx.doi.org/10.1021/jm3006146 | J. Med. Chem. XXXX, XXX, XXX−XXX

Table 1. Characterization and Properties of LRB Compounds 8, 9, and 27−30[a]

compd	solubility[b] (μM)	λ_{max}[c] (nm)	$\varepsilon_{\lambda max}$ (10^3 $M^{-1}\cdot cm^{-1}$)[c]	binding (nM)[d] K_i	functional activity (nM)[f] K_{act}	functional activity (nM)[f] K_{inact}
AVP				1.36 ± 0.45[e]	0.29 ± 0.05	
1	nd			2.68 ± 0.38		
2	nd			0.57 ± 0.18		0.096 ± 0.030
8o	nd	564	68	187.7 ± 24.7		163.6 ± 3.3
8p	3.4 ± 0.2	561	122	54.3 ± 6.6		16.7 ± 2.1
9o	nd	564	63	14.05 ± 1.72		2.12 ± 1.06
9p	2.1 ± 0.1	561	107	4.0 ± 0.7		1.96 ± 0.34
27	2.1 ± 0.2	561	74	25.3 ± 2.5		3.80 ± 0.36
28	3.1 ± 0.1	561	78	7.6 ± 0.7		0.66 ± 0.12
29	3.7 ± 0.3	561	106	12.7 ± 0.7		2.03 ± 0.04
30	6.2 ± 0.5	561	67	16.8 ± 1.0		8.91 ± 0.49

[a]Results are expressed as mean ± SEM of three separate experiments performed in triplicate. [b]The solubility was measured in a pH 7.4 HEPES buffer after 24 h of incubation at 22 °C. [c]The absorption parameters were measured in methanol. [d]The inhibition constants (K_i) of fluorescent compounds for the human vasopressin V_2R were determined on CHO cell membranes by competition binding assays (displacement of radioactive [^{3}H]AVP). [e]The affinity of AVP was directly determined in saturation binding assays using [^{3}H]-AVP as described before and led to the calculation of a [^{3}H]-AVP K_d.[39] [f]The K_{act} and K_{inact} constants of the novel ligands were determined using CHO cells stably expressing the V_2R and by measuring the accumulation of cAMP.[18]

which was reacted in the presence of 4-DMAP and pyridine to provide **25** in 72% yield. Finally, the conversion of the benzazepinone **25** into the amino-benzazepine **26** was efficiently achieved by reductive amination in the presence of NH_4OAc and $NaBH_3CN$. Microwave irradiations enabled to decrease the time of the reaction from 3 h to 2 × 5 min. Compound **26** was thus obtained in 33% overall yield for the five steps.

The introduction of *p*-LRB spacers **15**, **17**, and **18** was performed using PyBOP in situ activation[38] to furnish fluorescent probes **28**, **29**, and **30** in 50%, 67%, and 40% yields, respectively. Compound **27** was obtained by direct sulfonylation of **26** with *p*-LRB sulfonyl chloride in the presence of 4-DMAP in 62% yield. Both the purity and the identity of *p*-LRB labeled benzazepines **27**−**30** were confirmed by ^{1}H and ^{13}C NMR, liquid chromatography mass spectrometry (LC-MS), and high resolution mass spectrometry (HRMS).

Spectroscopic properties of LRB derivatives **8o**, **8p**, **9o**, **9p**, and **27**−**30** were examined in methanol (Table 1). They display similar maximum emission (ortho isomer, 564 nm; para isomer, 561 nm). However, the molar extinction coefficients ($\varepsilon_{\lambda max}$) are significantly different from the theoretical LRB sulfonyl chloride value (88000 $M^{-1}\cdot cm^{-1}$ in MeOH). Thus, for the homogeneous set of compounds **8** and **9**, the $\varepsilon_{\lambda max}$ of the para isomers (**8p**, 122000 $M^{-1}\cdot cm^{-1}$; **9p**, 107000 $M^{-1}\cdot cm^{-1}$) was found to be higher than that for the ortho isomers (**8o**, 68000 $M^{-1}\cdot cm^{-1}$; **9o**, 63000 $M^{-1}\cdot cm^{-1}$). On the other hand, *p*-LRB isomers **27**, **28**, and **30** exhibit a lower $\varepsilon_{\lambda max}$ values (74000, 78000, and 67000 $M^{-1}\cdot cm^{-1}$, respectively) than **8p** and **9p**. These results show that the $\varepsilon_{\lambda max}$ depends on the position of LRB functionalization (para or ortho) but also on the length and the nature of the spacers.

The solubility of *p*-LRB compounds was determined in a pH 7.4 HEPES buffer (Table 1). Compounds **8p**, **9p** and **27** exhibit a low solubility ranging from 2.1 to 3.4 μM. Unlike the results described in the literature,[25−27] the incorporation of spacers containing aqueous soluble piperazine or PEG moieties has only a low impact on the global solubility of *p*-LRB compounds **29** and **30** (3.7 and 6.2 μM, respectively).

Preparation of Fluorescein (Fluor), DY647, and Lumi4-Tb Labeled Ligands for TR-FRET Applications. All the fluorescent compounds were obtained following a solution-phase approach (Scheme 4). The key step was the

Scheme 4. Synthesis of the Spacers for Solution-Phase "Click" Chemistry[a]

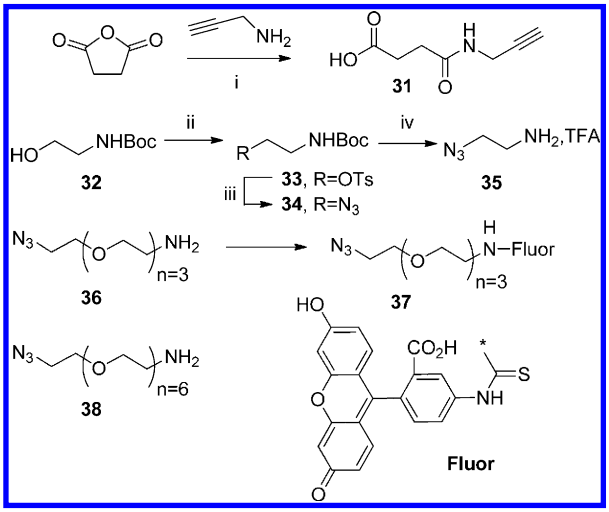

[a]Reagents: (i) 4-DMAP, CH_2Cl_2; (ii) TsCl, Et_3N, CH_2Cl_2; (iii) NaN_3, DMF; (iv) TFA/CH_2Cl_2.

Cu^I-catalyzed 1,3-dipolar cycloaddition between benzazepine acetylene **39** and different azido spacers of various chemical nature and lengths.[30] Compound **39** was obtained by coupling amino-benzazepine **26** with propargyl acid **31** following a PyBOP in situ activation. Compound **31** was readily prepared by condensation of an excess of propargylamine with succinic anhydride in the presence of a catalytic amount of 4-DMAP. Prior to the synthesis of Fluor labeled benzazepine **40**, Fluor-$(PEG)_3$-azido **37** was synthesized by reacting fluorescein

dx.doi.org/10.1021/jm3006146 | J. Med. Chem. XXXX, XXX, XXX−XXX

Scheme 5. Synthesis of Fluorescent Compounds 40, 44−49 for TR-FRET Applications[a]

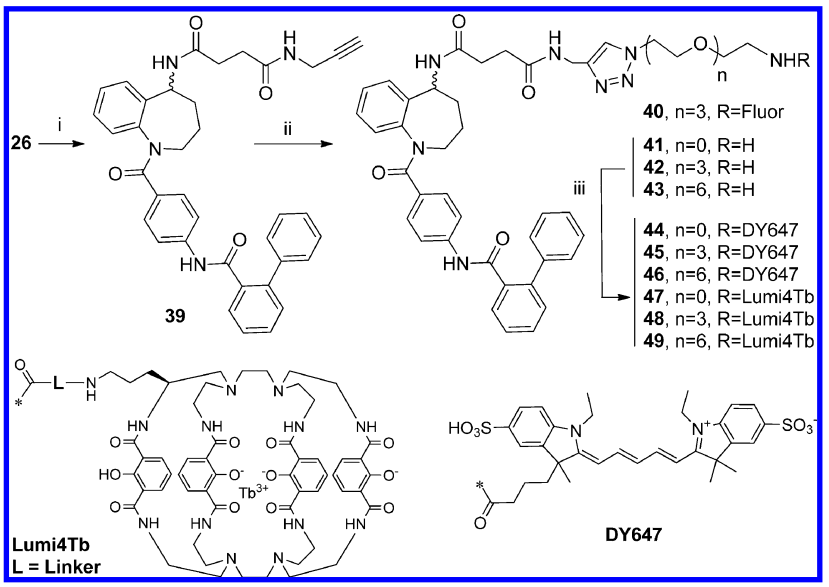

[a]Reagents: (i) **31**, PyBOP, Hünig's base, DMF; (ii) sodium ascorbate, $CuSO_4$, $5H_2O$, TBTA, DMF/H_2O (9/1); (iii) RCONHS, DMSO, Hünig's base.

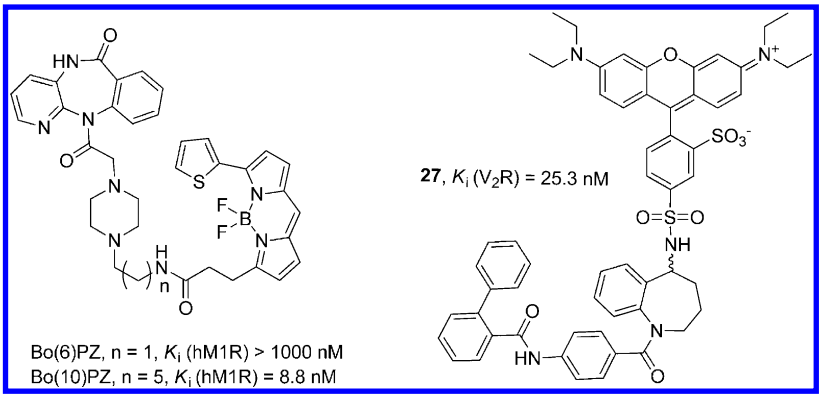

Figure 3. Chemical structures of Bodipy labeled pirenzepine (Bo(6)Pz and Bo(10)Pz, (Ilien et al.[8]) and LRB labeled benzazepine **27**.

isothiocyanate with amino-$(PEG)_3$-azido **36** in the presence of Et_3N in DMF (87% yield). The subsequent "Click" chemistry with acetylene **39** was achieved in the presence of sodium ascorbate and $CuSO_4$. The rate of conversion was best accomplished in the presence of catalytic amount of tris[(1-benzyl-1*H*-1,2,3-triazol-4-yl)methyl]amine, (TBTA) in a DMF/H_2O (9/1) mixture. Following these experimental conditions, Fluor labeled benzazepine **40** was isolated by RP-HPLC in a low 24% yield.

Therefore, for the more expensive dyes such as DY647 and Lumi4-Tb, the incorporation was envisaged at the very last stage of the process. Thereby, "Click" reaction was first conducted with amino-azido spacers **35**, **36**, and **38** and further functionalized with either DY647 or Lumi4-Tb. 2-Azidoethan-1-amine **35** was synthesized in a three-step process from commercially available *N*-Boc-ethanolamine **32**, which was converted into the corresponding tosylate **33** (Scheme 4). The nucleophilic substitution with NaN_3 enabled the formation of azido **34**, which was treated in the presence of TFA to provide expected 2-azidoethan-1-amine **35** in 68% overall yield (three steps).

"Click" chemistry performed with the three spacers **35**, **36**, and **38** furnished the functionalized amino-benzazepines **41**, **42**, and **43** ready to be acylated by succinimic ester of DY647 or Lumi4-Tb to lead fluorescent probes **44−49** (Scheme 5).

Receptor Binding and Function Assays of Fluorescent Probes. The affinity of labeled compounds **8**, **9**, **27−30**, **40**, and **44−49** for human V_2R was determined by competition experiments against [^{3}H]-AVP as described previously.[39] The affinity of nonfluorescent compounds **1** and **2** for the human receptor was found to be close to that published in the literature on rabbit kidney membranes (K_i = 2.68 vs 7.2 nM for **1** and K_i = 0.57 vs 7.6 nM for **2**). For the LRB analogues (Table 1), the biphenyl derivatives **9o,p** display a better affinity than the *o*-toluyl compounds **8o,p**. It is also important to note that despite the incorporation of the bulky dye onto the benzazepine analogues, the affinities of the resulting fluorescent constructs for V_2R are still in the nanomolar range. Nevertheless, the orientation of the LRB dye has an influence on the V_2R binding affinity. Indeed, the *para*-LRB isomers displayed on average a 3-fold better affinity than the corresponding *ortho*-LRB isomers. Finally, for the set of LRB molecules, the highest affinity for V_2R was obtained with the para isomer of the biphenyl derivative **9p** (K_i = 4 nM). Very interestingly, this affinity is in the range of that of the endogenous ligand AVP for

dx.doi.org/10.1021/jm3006146 | J. Med. Chem. XXXX, XXX, XXX−XXX

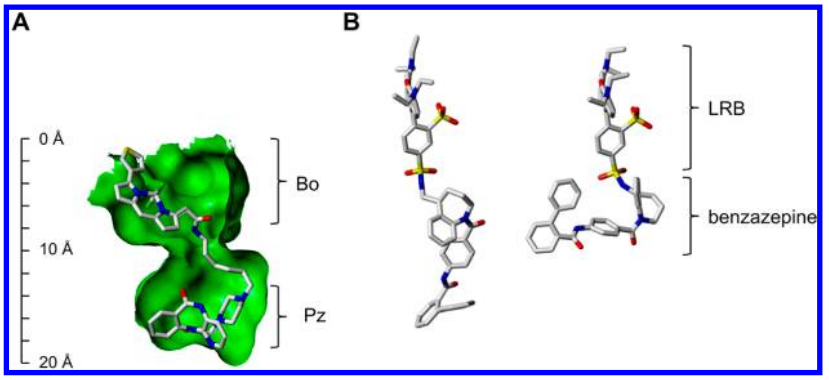

Figure 4. Three-dimensional models of fluorescent GPCR ligands. (A) Conformation of Bo(10)Pz as bound to M1R, whose transmembrane cavity is represented green solvent-excluded surface. (B) LRB benzazepine **27** in extended and folded conformations (left and right panels, respectively). Bo(10)Pz and LRB benzazepine **27** are represented using capped sticks colored according to CPK. All the panels are at the same scale.

Table 2. Determination of the Inhibition Constants of Fluorescent Compounds by Competition Experiments Using Radioactivity and TR-FRET Binding Methods[a]

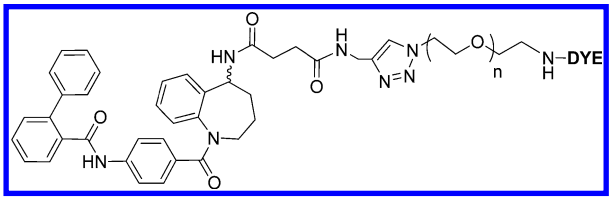

			binding		functional activity (nM)[c]	
compd	*n*	DYE	[^{3}H]AVP, K_i (nM)[b]	TR-FRET,[d] K_d (nM)	K_{act}	K_{inact}
40	3	fluor	26.1 ± 5.2	11.1 ± 2.2		0.78 ± 0.21
44	0	DY647	5.69 ± 1.05	1.38 ± 0.56		0.1 ± 0.001
45	3	DY647	9.02 ± 0.24	2.33 ± 1.23		0.1 ± 0.02
46	6	DY647	14.22 ± 0.19	2.53 ± 1.19		0.54 ± 0.1
47	0	Lumi4-Tb	5.86 ± 0.83	2.10 ± 0.87		0.42 ± 0.12
48	3	Lumi4-Tb	16.1 ± 2.5	3.17 ± 0.78		1.36 ± 0.1
49	6	Lumi4-Tb	30.65 ± 5.03	6.20 ± 2.13		3.64 ± 0.86

[a]Results are expressed as mean ± SEM of three independent separate experiments performed in triplicate. [b]The inhibition constants of fluorescent compounds for the human vasopressin V_2R were determined on CHO cell membranes by competition binding assays (displacement of radioactive [^{3}H]AVP).[39] [c]The K_{act} and K_{inact} constants of the novel ligands were determined using CHO cells stably expressing the V_2R and by measuring the accumulation of cAMP.[18] [d]The K_d constants of fluorescent ligands were directly determined by time-resolved FRET saturation experiments using HEK 293T cells transiently expressing SNAP-tagged V_2R and increasing concentrations of fluorescent ligands.[48] Nonspecific binding was determined in the presence of an excess of the unlabeled corresponding ligands (10 μM).

the human V_2R (K_i = 1.36 nM) measured in the same cell line.[39]

Influence of the Length and the Nature of the Spacers. Starting from the most potent *p*-LRB biphenyl benzazepine **9b**, we envisaged to modulate both the length and the nature of the spacer to investigate their influence on the affinity for V_2R. The incorporation of three different spacers such as an amino caproyl ester (compound **27**), the corresponding piperazinyl (compound **28**), or the much longer $(PEG)_3$ spacers (compound **29**) did not permit improvement of the affinity of the ligands for V_2R (K_i = 7.6, 12.7, and 16.9 nM, respectively) compared to the more potent *p*-LRB biphenyl benzazepine **9b** (K_i = 4.0 nM). More surprisingly, compound **27** obtained by direct incorporation of *p*-LRB into the amino-benzazepine scaffold retains a nanomolar affinity for V_2R (K_i = 25 nM). This result differs from the strategy generally used to design fluorescent nonpeptidic ligands of GPCRs, which consists in introducing a functionalized chain between the pharmacophore and the fluorophore to relax the constraints of the pharmacophore-binding site.[40] For instance, on the acetylcholine muscarinic M1 receptor antagonist telenzepine, Jacobson et al. have shown that a six methylene spacer between the pharmacophore and the fluorophore was the minimum length required to retain affinity between receptor and ligands.[41] For the same receptor, Ilien et al. have described the synthesis of various fluorescent pirenzepine analogues.[8] Provided the spacer is long enough (>10 methylenes, Bo(10)PZ, Figure 3) and whatever its nature (PEG or isopeptidic), the fluorescent ligands exhibit nanomolar affinities for the human muscarinic M1 receptor (M1R). In our case, the biological evaluation of compound **27** shows that the absence of spacer is not detrimental for the affinity (Figure 3).

The modeling of the three-dimensional structure of the receptors and their ligands provides insights into the required length for the spacer between the orthosteric ligand and the fluorophore. An accurate model of M1R was built based on the crystal structure of its close homologue, the muscarinic M3 receptor.[42] Its transmembrane cavity has a characteristic shape

dx.doi.org/10.1021/jm3006146 | J. Med. Chem. XXXX, XXX, XXX−XXX

Table 3. Determination of the Inhibition Constants of the Fluorescent Ligands for the Vasopressin and Oxytocin Receptors[a]

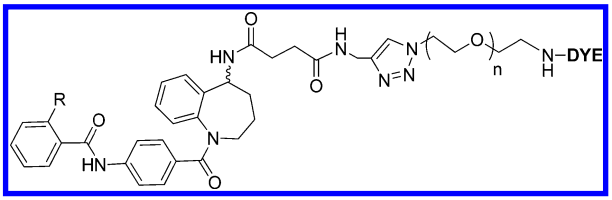

				binding[a] (K_i, nM)			
compd	*n*	DYE	R	V_2	V_{1a}	V_{1b}	OT
AVP				1.48 ± 0.08	0.7 ± 0.17	0.49 ± 0.06	1.65 ± 0.49
2				0.57 ± 0.18	2.74 ± 0.19		109 ± 34
8o	3	*o*-LRB	Me	187.7 ± 24.7	>10000	>10000	307 ± 18
8p	3	*p*-LRB	Me	54.3 ± 6.6	>10000	>10000	495 ± 101
9o	3	*o*-LRB	Ph	14.05 ± 1.72	>10000	>10000	>10000
9p	3	*p*-LRB	Ph	4.0 ± 0.7	>10000	>10000	>10000
40	3	fluor	Ph	26.1 ± 5.2	>10000	>10000	665 ± 47
44	0	DY647	Ph	5.69 ± 1.05	621 ± 65	>10000	184 ± 31
45	3	DY647	Ph	9.02 ± 0.24	1753 ± 338	>10000	808 ± 61
47	0	Lumi4-Tb	Ph	5.86 ± 0.83	180 ± 34	>10000	155 ± 8
48	3	Lumi4-Tb	Ph	16.1 ± 2.5	750 ± 89	>10000	304 ± 70

[a]The inhibition constants of fluorescent compounds for the human vasopressin V_{1a}, V_{1b}, V_2, and oxytocin receptors were determined on CHO cell membranes by competition binding assays (displacement of radioactive [^{3}H]AVP). Results are expressed as mean ± SEM of three independent separate experiments performed in triplicate. A K_i > 10000 indicated that displacement of [^{3}H]AVP with each fluorescent compound at 10 μM led to no competition or to less than 50% inhibition.

due to a layer of aromatic residues conserved across muscarinic receptor subtypes that restricts the access to the orthosteric binding site and so defines a vestibule (Supporting Information, Figure S5). The automated docking of Bo(10)Pz into the M1R transmembrane cavity places the pirenzepine moiety in the orthosteric site near Asp105 (Asp3.32 according to Ballesteros–Weinstein numbering), whereas the Bodipy remains in the vestibule and stacked onto the Trp400 (Trp7.35) side chain. The size of the spacer in Bo(10)Pz determines the positioning of the fluorophore: if shorter than 10 atoms, the pirenzepine moiety would not reach its buried site because of steric hindrance between the fluorophore and the narrow gate between the orthosteric site and the vestibule.

In the modeled complex between Bo(10)Pz and M1R, the conformation of pirenzepine is extended, with the longest interatomic distance in the order of 12 Å (Figure 4A). In the low energy conformations of the biphenyl benzazepine moiety of compound **27**, the longest interatomic distance is comprised between 14 and 15 Å. As a consequence, the biphenyl benzazepine moiety of compound **27** is bulkier than pirenzepine, and therefore its binding site in V_2R is expected to be larger than the orthosteric site in M1. In support of this hypothesis, V_2R binds endogenous peptides like the chemokine receptor CXCR4[43] and opioid receptors[44] whose structures are known and whose transmembrane cavities are widely open and well accessible to ligands. The comparison of the size of compound **27** with the depth of transmembrane cavity, which is approximately 20 Å in M3, CXCR4, and opoid receptors, suggests that if the biphenyl benzazepine moiety deeply penetrates the cavity, the LBR moiety would be almost entirely outside of the cavity (Figure 4B, left panel). Any upper positioning in the transmembrane cavity of the biphenyl benzazepine is consistent with a large solvent accessibility of LRB, and this is even if compound **27** adopts a folded conformation (Figure 4B, right panel). A rough model of complex between human V_2R and compound **27** is provided as Supporting Information.

Influence of the Nature of the Fluorophores. With the aim of developing fluorescent ligands suitable for TR-FRET techniques, *p*-LRB dye of compound **9p** was replaced by Lumi4-Tb, fluorescein, or DY-647. Table 2 shows that the fluorophore slightly contributes to the affinity for V_2R in the following order: *p*-LRB (**9p**, 4 nM) > DY647 (**45**, 9 nM) > Lumi4-Tb (**48**, 16 nM) > fluorescein (**40**, 26.1 nM). In an attempt to further improve the affinity of ligands **48** and **45**, the fine-tuning of the length of the spacer (*n* = 0, 3, 6, Table 2) was performed. The affinity decreased along with the length of the spacer. Thus, compound **46** and **49** containing an ethylene-$(PEG)_6$ spacer (K_i = 14.2 and 30.6 nM, respectively) displayed a loss of 2.5-fold and 5.2-fold in affinity compared to compound **44** and **47** containing an ethylene spacer (K_i = 5.6 and 5.8 nM, respectively).

Selectivity of the Fluorescent Probes. The selectivity of the ligands exhibiting the highest affinity for the various subtypes of human AVP/OT receptors was also investigated (Table 3). The nonfluorescent ligand **2** displays affinities for V_2R but also V_{1a} and OT receptors (K_i = 0.57/2.74/109 nM, respectively). The incorporation of a fluorescent dye through a spacer at the 5-amino position of benzazepine slightly decreases the affinity of the resulting molecule for V_2R, whereas it severely disturbs $V_{1a}R$, $V_{1b}R$, and OTR binding affinities. Thus, LRB analogues **9o,p** exhibit a strong affinity and selectivity for V_2R, suggesting an adequacy between the structure of the LRB-labeled ligands and the binding pocket of the V_2R. These results are in accordance with those described for 5-amino substituted benzazepines such as OPC-31260 (Figure 2).[23] Interestingly, ligands **8o,p** containing *o*-toluyl group are much less selective for the V_2R compared to ligands **9o,p** because they still display a medium affinity for OT. Thus, compound **9p** represents the first selective fluorescent nonpeptidic antagonist for V_2R described to date.

dx.doi.org/10.1021/jm3006146 | J. Med. Chem. XXXX, XXX, XXX–XXX

Changing the nature of the fluorophore was found also to have an influence on the affinity of the ligands for $V_{1a}R$ and OTR. Thus, the inhibition constant for Fluor ligand **40** was 665 nM for OTR with still a 25-fold V_2R binding selectivity. Nevertheless, the incorporation of DY647 and Lumi4-Tb is less detrimental for the affinity of the fluorescent ligands for $V_{1a}R$ and OTR. A better selectivity was obtained for compounds bearing DY647 than those bearing Lumi4-Tb. The high-affinity V_2R compounds **44** (DY647, K_i = 5.69 ± 1.05 nM) and **47** (Lumi4-Tb, K_i = 5.86 ± 0.83 nM) show a 109- and 30-fold in $V_{1a}R$ selectivity and a 32- and 26-fold in OTR selectivity, respectively.

The functional activity of all the fluorescent ligands was evaluated by the measurement of cyclic adenosine monophosphate (cAMP) accumulation following cell incubation with the fluorescent ligands at a concentration of 100-fold K_i (Tables 1 and 2). For all fluorescent probes, no significant increase in accumulation of second messengers was detected, whereas AVP displayed full agonist properties and a high potency (K_{act} = 0.29 nM). This result indicates that the fluorescent ligands are devoid of intrinsic agonist activity. Moreover, all fluorescent ligands fully inhibited AVP-induced cAMP accumulation in a dose-dependent manner, highlighting their antagonistic character. The inhibition constant values for **44** and **47** (K_{inact} = 0.069 and 0.42 nM, respectively) were close to that for nonfluorescent ligand **2** (K_{inact} = 0.096 nM). Interestingly, regardless of the nature of the dye, the length and the chemical nature of the spacers, the antagonist properties of all the fluorescent ligands for V_2R were not affected. With the exception of **8o**, all novel fluorescent compounds (**8p**, **9o**, **9p**, **27**−**30**, and **40**−**49**) display potency toward inhibition of AVP-induced cAMP accumulation in the nanomolar or subnanomolar range.

Fluorescent-Based Assay for V_2R. During the last decades, the domain of application of fluorescent ligands has been extended. While fluorescent analogues were essentially used to label receptor to study their localization, they become suitable tools to develop binding assays or to identify new receptor complexes. The above study has shown that LRB analogue **9p** combined high affinity and selectivity for V_2R with very potent antagonist properties. This ligand in hand, we decided to develop a FRET-based assays for HTS on V_2R by using an enhanced green fluorescent protein (EGFP)-fused V2 receptor, following the same strategy then previously described.[45] However, the low signal-to-noise ratio resulting from the intrinsic fluorescence of cells and the overlap between the emission spectra of FRET donors and acceptors precluded the development of a sensitive and specific assay (data not shown). To overcome these limitations, we turned our attention to the TR-FRET approach based on the use of terbium cryptate, Lumi4-Tb,[31] as a donor and fluorescein or DY647 as acceptors. Such technique usually offers a higher signal-to-noise ratio than classic FRET for two mains reasons. First, the long lifetime of the terbium enables measurement of FRET emission when all natural fluorophore have switched off and, second, this donor fluorophore has a very limited emission at 665 nm where the acceptor emission is measured.[46] We performed TR-FRET-based saturation experiments with analogues **44**−**49** and receptor labeled with the SNAP-tag approach.[47] SNAP-tagged receptors were labeled either with a Lumi4-Tb donor (SNAP-Lumi4-Tb) or d2 acceptor (SNAP-red) derivatized benzylguanine substrates depending on the nature of the ligands, either acceptor (**44**−**46**) or donor (**47**−**49**), respectively. Saturation curves were obtained when plotting specific FRET signal in function of fluorescent analogue concentration (Figure 5). As shown in Table 2, the resulting dissociation constants were in accordance with those determined by radioactive assays validating the TR-FRET assays with nonpeptidic V_2 fluorescent ligands.

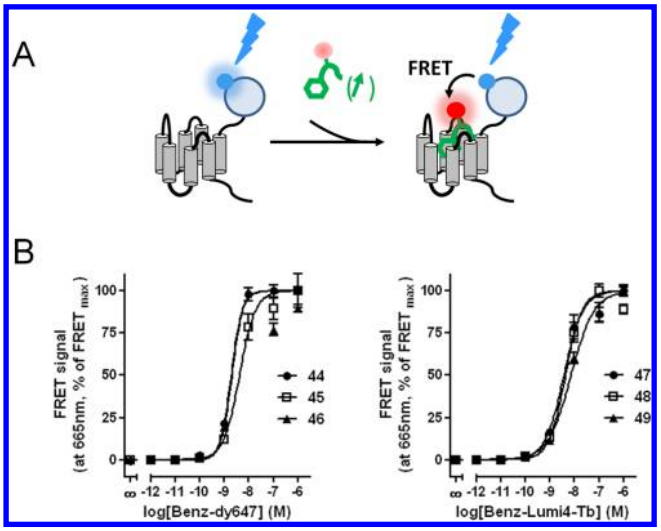

Figure 5. Time-resolved FRET-based saturation experiments with analogues **44**−**49** and receptor labeled with the SNAP-tag approach. (A) Cells expressing a receptor of interest fused to SNAP-tag are incubated in presence of a fluorescent substrate to label the receptor. Cells were then incubated in the presence of increasing concentration of fluorescent ligands. Fluorophores of the SNAP-tag substrates and of the ligands are chosen to be compatible with time-resolved FRET strategy. (B) Fluorescence intensity of the acceptor is plotted in function of the concentration of the tracer.

Then, we performed competition experiments to test the relevance of such fluorescent ligands in pharmacological assays. The principle of the competition assays is illustrated in Figure 6A. As proof-of-concept, we used **45** and **46** as tracers and vasopressin as competitor. Competition curve with **45** is illustrated in Figure 6B. Inhibition constants (K_i) for AVP determined by such competition assays with **45** and **46** are 1.93 and 0.83 nM, respectively, in agreement with its K_d (1.36 nM) determined by saturation with [^{3}H]AVP.

Cell-Surface $V_{1a}R$−V_2R Dimerization Study. In the last two decades, the concept of receptor oligomerization emerged. Many studies have described the propensity of GPCRs to form dimers or higher-order oligomers resulting from the interaction of one receptor subtype (homomers) or various receptors (heteromers). The capacity of one receptor to interact with various GPCRs can be at the origin of variations in the pharmacological profile, and it is therefore of interest in drug screening. Nevertheless, all dimeric combinations of about 400 GPCRs expressed in human and excluding odorant receptors, do not exist. Therefore one crucial challenge is to identify in native tissues dimers that have potentially a physiological function and which are potentially interesting therapeutic targets. Recently, we brought evidence of the existence of OTR homodimers in mammary glands in performing TR-FRET between fluorescent ligands bound to a receptor dimer.[14] The development of various selective fluorescent ligands opens new possibilities to detect heterodimers. We tested the strategy on V_{1a} and V_2 receptors coexpressed in COS-7 cells (Figure 7)

dx.doi.org/10.1021/jm3006146 | J. Med. Chem. XXXX, XXX, XXX−XXX

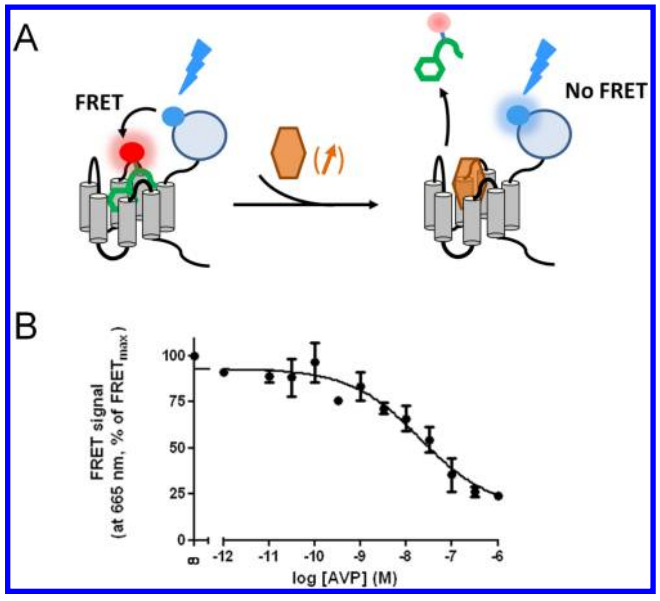

Figure 6. Competition assays with **45** as tracer and vasopressin as competitor. (A) Cell expressing vasopressin V_2 receptor have been labeled using the SNAP-tag technology and were incubated in the presence of **45** (20 nM) and increasing concentration of AVP. (B) Fluorescence intensity measured at 665 nm was plotted as a function of AVP concentration. The K_i determined with Cheng–Prussof equation is 1.93 nM.

using [Lys^8(Eu–PBBP)]PVA and [Lys^8(Alexa-647)]PVA[14] to label V_{1a} receptor and **44** and **47** to label V_2 receptor, respectively. As expected, V_{1a} receptor homodimers were only detected on cells expressing V_{1a} or V_{1a}/V_2 receptors with [Lys^8(Eu–PBBP)]PVA and [Lys^8(Alexa-647)]PVA as donor and acceptor ligands. In the same manner, V_2 receptor homodimers were only detected on cells expressing V_2 or V_{1a}/V_2 receptors with **44** and **47**. Finally, V_{1a}/V_2 heterodimers were only detected in cells in which V_{1a} and V_2 receptors are coexpressed and with [Lys^8(Eu–PBBP)]PVA and **44** on the one hand or [Lys^8(Alexa-647)]PVA and **47** on the other hand. Therefore, the results strongly support the usefulness of specific ligands to detect heterodimers in cells.

In this paper, we report the first selective fluorescent nonpeptidic antagonists for AVP V_2R subtype. "Click" chemistry performed either on solid-phase or in solution gave a rapid and straightforward access to those fluorescent molecules. It is noteworthy that the incorporation of a dye on the starting benzazepine scaffold makes the resulting fluorescent probes much more selective for V_2R, compared to V_{1a}R, V_{1b}R, and OTR. To date, *p*-LRB probe **9p** is the most selective and potent fluorescent nonpeptidic antagonist for V_2R. although we have not succeeded in the development of a GFP-FRET-based assay, we anticipate that this compound will find application in the field of cell imaging for receptor localization, trafficking studies, or anisotropy technologies. Furthermore, DY647 and Lumi4-Tb probes were found to be useful tools for the development of V_2R TR-FRET-based assay readily

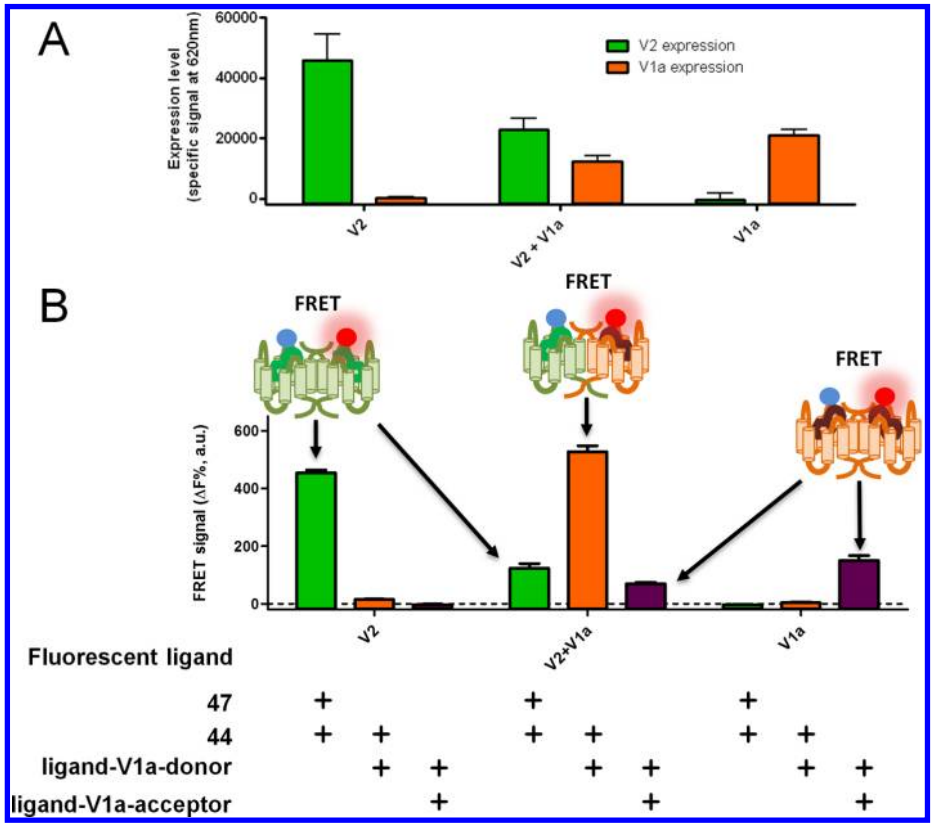

Figure 7. Detection of V_{1a}–V_2 heteromers at the surface of COS-7 cells. (A) Expression of V_2, V_{1a}, or both receptors in Cos7 cells. (B) Dimerization signal of V_2, V_{1a}, or both receptors expressed in Cos7 cells. Cos7 cells expressing either V_2 or V_{1a} or both receptors were incubated in the presence of a mix of fluorescent ligands as indicated on the panel. V_2 and V_{1a} receptor homodimers were only detected in cells expressing these receptors in the presence of their cognate fluorescent ligands indicating the specificity of the ligand. The V_2/V_{1a} receptor heterodimers were only detected in cells expressing both receptors using a combination of V_2 and V_{1a} fluorescent ligands.

dx.doi.org/10.1021/jm3006146 | J. Med. Chem. XXXX, XXX, XXX–XXX

amenable to HTS. Taking advantage of their selectivity, the same compounds were also demonstrated to represent powerful tools to study $V_{1a}R-V_2R$ dimerization at the cell surface. These ligands present great advantages over peptides to be more stable in vivo, paving the way to GPCR oligomerization studies in native tissues.

EXPERIMENTAL SECTION

General Methods. Reagents were obtained from commercial sources and used without any further purification. Lissamine rhodamine B sodium sulfonate (Acid Red 52 sodium salt) was purchased from TCI Europe (Zwijndrecht, Belgium), Lissamine Rhodamine B sulfonyl chloride (mixed isomers) from Acros Organics (Halluin, France), and fluorescein 5-isothiocyanate from Sigma (Saint Quentin Fallavier, France). (±)-5-amino-1-*tert*-butoxycarbonyl-2,3,4,5-tetrahydro-1*H*-benzo[*b*]azepine, Lissamine-$(PEG)_3$-azido **7**, SPOrT resin, and compounds **8o,p** were obtained as previously described.[22,33] Lumi4-Tb-NHS, SNAP-Lumi4-Tb, SNAP-RED, and cAMP dynamic kit were purchased from Cisbio Bioassays (Codolet, France) and DY647-NHS from Dyomics GmbH (Jena, Germany). Thin-layer chromatography was performed on silica gel $60F_{254}$ plates. Flash chromatography was performed on silica gel (40 μm, Grace) or RP18 (25−40 μm, Merck) prepacked columns on a SPOT II ultima from Armen. ^{1}H NMR spectra were recorded at 400 MHz on a Bruker Advance spectrometer. Chemical shifts are reported in parts per million (ppm), and coupling constants (*J*) are reported in hertz (Hz). Analytical reverse-phase high performance liquid chromatography (RP-HPLC) separations were performed on a C18 Agilent Eclipse XDB (5 μm, 4.6 mm × 150 mm) using a linear gradient (90% A for 2 min and then 10% to 100% B in 15 min, flow rate of 1 mL·min^{-1}) of solvent B (100% CH_3CN, 0.1% TFA, v/v) in solvent A (100% H_2O, 0.1% TFA, v/v). Detection was set at 220 and 254 nm. Purified final compounds eluted as single and symmetrical peaks (thereby confirming a purity of ≥95%) at retention times (t_R) given below. Their identity was determined by high resolution mass spectra (HRMS), which were acquired on a Bruker MicroTof mass spectrometer, using electrospray ionization (ESI) and a time-of-flight analyzer (TOF).

General Procedure for the Solid-Phase "Click" Chemistry. Resin-bound alkyne **5** or **6** (46 μmol) was preswollen in a DMF/piperidine (4/1, v/v) mixture. In two separated vials, CuI (44.3 mg, 230 mmol) and Lissamine-$(PEG)_3$-azido (105.8 mg, 139 μmol) were dissolved in DMF/piperidine (4/1, v/v, 825 μL) using an ultrasonic bath. Both solutions were mixed altogether and placed again for 5 min in an ultrasonic bath. The resulting mixture (1.65 mL) was added to preswollen resin-bound alkyne. Following shaking for 6 h at 30 °C, the resin was washed successively with 4/1 (by vol) DMF/piperidine (3×), DMF (3×), CH_2Cl_2 (3×), CH_2Cl_2/MeOH (3×), MeOH (3×), and CH_2Cl_2 (3×) and dried in vacuo.

***ortho*- and *para*-LRB Labeled Compounds 9o,p.** Resin **6** (120 μmol), was submitted to the "click" chemistry protocol in the presence of *o,p*-LRB azido **7** (161 mg, 210 μmol): A subsequent deprotection and cleavage in TFA/H_2O (95:5) gave access to compounds **9o,p**. Both ortho **9o** and para isomers **9p** were isolated by RP-HPLC on a C18 Symmetry Shield column.

*ortho-LRB Labeled Compound (**9o**, 25 mg, 26%).* ^{1}H NMR ($CDCl_3/CD_3OD$ 9/1, 300 MHz): δ 8.53 (d, *J* = 1.5 Hz, 1H), 8.12 (dd, *J* = 8.1 and 1.5 Hz, 1H), 7.75 (bs, 1H), 7.39 (d, *J* = 8.1 Hz, 2H), 7.32−6.96 (m, 11H), 6.83 (bt, *J* = 7.5 Hz, 1H), 6.76 (dd, *J* = 9.3 et 2.4 Hz, 2H), 6.64 (bs, 2H), 6.50 (d, *J* = 7.5 Hz, 1H), 5.25 (bdd, *J* = 11.0 and 3.0 Hz, 1H), 4.46 (bs, 1H), 4.36 (bs, 2H), 4.29 (bt, *J* = 5.0 Hz, 2H), 3.96−3.80 (m, 8H), 3.69 (t, *J* = 4.8 Hz, 2H), 3.60−3.36 (m, 9H), 3.23 (bs, 3H), 2.95 (t, *J* = 5,1 Hz, 1H), 2.63−2.48 (bs, 4H), 2.3 (s, 3H), 2.0−1.80 (bs, 2H), 1.40−1.60 (bs, 2H), 1.25 (m, 12 H). ^{13}C NMR ($CDCl_3/CD_3OD$ 9/1, 75 MHz) δ 173.0, 172.6, 170,0, 169.4, 157.7, 156.1, 155.6, 148.5, 141.0, 140.6, 140.1, 138.6, 136.4, 135.9, 132.1, 131.5, 130.9, 130.7, 130.0, 129.7, 129.5, 128.3, 127.6, 127.5, 126.8, 125.8, 125.6, 124.2, 123.9, 118.8, 114.0, 95.9, 70.3, 70.1, 70.0, 69.5, 69.1, 50.5, 50.1, 48.0, 47.9, 42.9, 34.7, 31.4, 31.00, 25.2, 19.4, 12.4. RP-HPLC purity: >95%; t_R = 11.41 min. HRMS: calcd for $C_{72}H_{82}N_{10}O_{13}S_2$ 679.2747, found 679.2746 ((M + 2H$^+$)/2).

*para-LRB Labeled Compound (**9p**, 17 mg, 28%).* ^{1}H NMR ($CDCl_3/CD_3OD$ 9/1, 400 MHz) δ 8.63 (bs, 1H), 7.91 (bd, *J* = 8.1 Hz, 1H), 7.74 (bs, 1H), 7.38 (bs, 2H), 7.32−6.96 (m, 11H), 6.83 (bt, *J* = 7.5 Hz, 1H), 6.71 (bd, *J* = 9.3, 2H), 6.60 (bs, 2H), 6.50 (d, *J* = 7.5 Hz, 1H), 5.14 (bd, *J* = 11.0 Hz, 1H), 4.48−4.24 (m, 5H), 3.84−3.68 (m, 10H), 3.58−3.36 (m, 9H), 3.23 (bs, 1H), 3.01 (bs, 1H), 2.91 (bt, *J* = 5,1 Hz, 1H), 2.89 (bs, 1H), 2.58−2.38 (m, 4H), 2.3 (s, 3H), 1.88−1.80 (bs, 2H), 1.58−1.44 (bs, 2H), 1.18 (m, 12 H). ^{13}C NMR ($CDCl_3/CD_3OD$ 9/1, 100 MHz) δ 176.4, 175.9, 173.4, 172.7, 172.13, 161.2, 160.7, 158.9, 150.1, 145.8, 144.0, 143.5, 142.0, 139.8, 139.3, 137.1, 136.2, 134.2, 134.1, 133.7, 132.9, 131.6, 131.0, 130.9, 130.2, 130.1, 159.0, 127.6, 12.2, 117.5, 117.0, 99.1, 73.7, 73.5, 73.0, 72.5, 53.9, 53.6, 50.0, 49.6, 49.2, 46.3, 38.1, 34.9, 34.3, 28.6, 22.7, 15.7, 11.8. RP-HPLC purity: >95%; t_R = 11.50 min. HRMS for $C_{72}H_{82}N_{10}O_{13}S_2$ 679.2747, found 679.2740 ((M + 2H$^+$)/2).

Methyl 4-([1,1′-Biphenyl]-2-ylcarboxamido)benzoate (21). To a stirred solution of 2-biphenyl carboxylic acid (1 g, 5.0 mmol) in anhydrous CH_2Cl_2 (2.5 mL) at 0 °C under argon was added dropwise thionyl chloride (1.9 mL, 25 mmol) in the presence of a catalytic amount of dry DMF. Following 30 min stirring at 0 °C and then 3 h at room temperature, the mixture was concentrated in vacuo. The resulting solid dissolved in anhydrous CH_2Cl_2 (5 mL) was added dropwise to a solution of methyl 4-aminobenzoate (378 mg, 2.5 mmol) in CH_2Cl_2 (4 mL) and Hünig's base (860 μL, 5.0 mmol). After 15 min at 0 °C, the mixture was allowed to warm to room temperature and stirred for a further 2 h. The organic layer was washed, sequentially, with water, an aqueous citric acid solution (10%), an aqueous solution of 1 M NaOH, and water, dried with Na_2SO_4, and concentrated under reduced pressure. Following precipitation in EtOAc, compound **21** was obtained as a white powder (774 mg, 93%). R_f = 0.60 (heptane/EtOAc, 1/1, v/v); mp 150−152 °C. ^{1}H NMR (300 MHz, $CDCl_3$): δ 7.85−7.93 (m, 3H), 7.35−7.60 (m, 8H), 7.17 (d, *J* = 8.4 Hz, 2H), 7.05 (sl, 1H), 3.87 (s, 3 H). ^{13}C NMR (75 MHz, $CDCl_3$): δ 167.1, 166.5, 141.7, 139.7, 139.6, 134.7, 131.0, 130.6, 130.4, 129.7, 129.1, 128.8, 128.3, 128.0, 125.6, 118.7, 52.0.

4-([1,1′-Biphenyl]-2-ylcarboxamido)benzoic Acid (22). A stirred solution of compound **21** (500 mg, 1.51 mmol) in a 6 N HCl/AcOH (1/1, v/v, 50 mL) mixture was refluxed for 4 h. The resulting mixture was poured into ice-cold water solution to obtain compound **22** as a white powder (500 mg, 1.51 mmol). R_f = 0.5 (heptane/EtOAc 1/1); mp 236−238 °C. ^{1}H NMR (200 MHz, DMSO-d_6): δ 7.20−7.75 (m, 11H), 7.84 (d, *J* = 8.6 Hz, 2H), 10.54 (s, 1H), 12.46 (bs, 1H). ^{13}C NMR (75 MHz, DMSO-d_6): δ 168.2, 166.9, 143.1, 140.9, 139.9, 139.3, 136.7, 130.2, 130.0, 128.3, 128.1, 127.8, 127.3, 127.2, 125.4, 118.8. RP-HPLC purity: 93%, t_R = 13.59.

***N*-(4-(5-Oxo-2,3,4,5-tetrahydro-1*H*-benzo[*b*]azepine-1-carbonyl)phenyl)-[1,1′-biphenyl]-2-carboxamide (25).** To a stirred solution of compound **22** (200 mg, 0.63 mmol) in CH_2Cl_2 (5 mL) was added thionyl chloride (142 μL, 1.94 mmol) with a catalytic amount of dry DMF. Following overnight stirring at room temperature, the mixture was concentrated in vacuo. The residue was dissolved in CH_2Cl_2 (5 mL) and dropwise added to a solution of 1,2,3,4-tetrahydro-5*H*-1-benzazepin-5-one **24** (78 mg, 0.48 mmol) in CH_2Cl_2 (2 mL) at 0 °C in presence of pyridine (117 μL, 1.45 mmol) and 4-DMAP (12 mg, 0.10 mmol). The mixture was stirred for 4 h, diluted in CH_2Cl_2 (5 mL), and washed, sequentially, with an aqueous 1 N HCl solution and a saturated solution of $NaHCO_3$. Following concentration under reduced pressure, the crude was purified by chromatography over silica gel column (heptane/EtOAc, 1/1, v/v) to provide compound **25** as a white powder (165 mg, 74%); R_f = 0.40 (heptane/EtOAc, 2/3, v/v); mp 128−130 °C. ^{1}H NMR (200 MHz, $CDCl_3$): δ 7.58−7.51 (m, 2H), 7.28−7.08 (m, 2H), 6.98−6.91 (m, 2H), 6.78 (t, *J* = 8.6 Hz, 3H), 6.65 (d, *J* = 8.6 Hz, 2H), 6.40 (dd, *J* = 7.0, 1.7 Hz, 1H), 3.18 (q, *J* = 7.1 Hz, 4 H), 2.56 (t, *J* = 6.3 Hz, 2H). ^{13}C NMR (75 MHz, $CDCl_3$): δ 202.2, 170.0, 167.4, 143.2, 139.8, 139.7, 135.0, 134.4, 133.1, 130.9, 130.7, 129.8, 129.5, 129.1, 129.0, 128.8, 128.2, 127.9, 118.8, 40.3, 29.8, 22.8. RP-HPLC purity: 94%; t_R = 14.39. ES-MS for $C_{30}H_{25}N_2O_3$ (M + H$^+$): calcd 461.18, found 461.09.

dx.doi.org/10.1021/jm3006146 | J. Med. Chem. XXXX, XXX, XXX−XXX

***N*-(4-(5-Amino-2,3,4,5-tetrahydro-1*H*-benzo[*b*]azepine-1-carbonyl)phenyl)-[1,1′-biphenyl]-2-carboxamide (26).** To a stirred solution of compound **25** (53 mg, 0.12 mmol) in MeOH (2.5 mL) was added NH_4OAc (532 mg, 6.91 mmol) and $NaBH_3CN$ (36 mg, 0.58 mmol). Following microwave irradiation (2 × 5 min at 100 °C, 1 bar), the mixture was washed, sequentially, with a saturated solution of $NaHCO_3$ and NaCl and concentrated in vacuo. The residue was purified by RP-HPLC then freeze-dried to provide compound **26** as a white powder (31 mg, 57%). R_f = 0.1 (EtOAc/MeOH/Et_3N, 9/1/0.01, v/v/v); mp 177−178 °C. ^{1}H NMR (400 MHz, DMSO-d_6): δ 10.30 (bs, 1H), 8.74 (bs, 2H), 7.58−7.53 (m, 2H), 7.49−7.44 (m, 2H), 7.39−7.29 (m, 9H), 7.14−7.09 (m, 3H), 6.76 (d, J = 7.1 Hz, 1H), 4.73 (bs, 1H), 4.58 (bs, 1H), 2.82 (t, J = 11.3 Hz, 1H), 2.19 (bs, 1H), 1.92 (bs, 1H), 1.65 (bs, 2H). ^{13}C NMR (75 MHz, CD_3OD): δ 171.3, 171.2, 142.7, 142.4, 141.5, 141.4, 137.8, 132.6, 131.5, 131.4, 130.1, 129.8, 129.6, 129.5, 129.1, 129.0, 128.7, 128.6, 125.7, 120.2, 53.3, 48.3, 36.7, 27.3. RP-HPLC purity: 91%; t_R = 12.51. HRMS for $C_{30}H_{28}N_3O_2$: calcd 462.2176, found 462.2171.

5-(*N*-(1-(4-([1,1′-Biphenyl]-2-ylcarboxamido)benzoyl)-2,3,4,5-tetrahydro-1*H*-benzo[*b*]azepin-5-yl)sulfamoyl)-2-(6-(diethylamino)-3-(diethyliminio)-3*H*-xanthen-9-yl)benzenesulfonate (27). To a stirred solution of compound **26** (12 mg, 0.03 mmol) in a CH_2Cl_2/DMF (1/1, v/v) mixture was added *p*-LRB sulfonyl chloride (23 mg, 0.04 mmol) in the presence of Hünig's base (23 μL, 0.13 mmol) and a catalytic amount of 4-DMAP. Following 1 h at room temperature, the resulting mixture was concentrated under reduced pressure. The residue was purified by flash chromatography on a C18 column (prepacked columns, 25−40 μm, Merck) using a linear gradient (95% C to 100% D in 30 min, flow rate of 15 mL·min^{-1}) of solvent D (100% CH_3CN) in solvent C (100% H_2O). After freeze-drying, compound **27** was obtained as a red powder (16 mg, 62%); mp 233−235 °C. ^{1}H NMR (400 MHz, $CDCl_3$): δ 8.92 (s, 1 H), 8.04 (d, J = 8.0 Hz, 1 H), 7.72 (s, 1 H), 7.55 (d, J = 7.9 Hz, 1 H), 7.38 (d, J = 7.3 Hz, 2H), 7.27−7.25 (m, 5 H), 7.19 (d, J = 8.2 Hz, 2 H), 7.12 (d, J = 8.2 Hz, 2 H), 7.02 (d, J = 8.2 Hz, 2 H), 6.96 (t, J = 10.5 Hz, 2 H), 6.81 (t, J = 7.5 Hz, 1 H), 6.64−6.57 (m, 5 H), 6.46 (d, J = 7.4 Hz, 1 H), 4.86 (d, J = 9.5 Hz, 1 H), 4.34 (t, J = 9.4 Hz, 1 H), 3.54−3.43 (m, 8 H), 3.00 (t, J = 9.4 Hz, 1 H), 2.09 (sl, 2 H), 1.83 (sl, 1 H), 1.23−1.18 (m, 12 H). ^{13}C NMR (75 MHz, $CDCl_3$): δ 167.5, 158.1, 158.0, 155.7, 140.3, 140.1, 137.6, 135.3, 133.8, 133.6, 133.5, 131.2, 130.6, 130.5, 130.2, 129.2, 129.1, 128.8, 128.8, 128.4, 127.9, 127.6, 127.5, 127.4, 126.5, 118.9, 114.5, 114.5, 113.8, 95.7, 54.6, 46.5, 46.0, 33.2, 25.1, 12.8. RP-HPLC purity: 95%; t_R = 15.09. HRMS for $C_{57}H_{56}N_5O_8S_2$: calcd 1002.3570, found 1002.3568.

General Procedure for the Coupling of *para*-LRB Spacers 15, 17, and 16. To a solution of *p*-LRB spacer carboxylic acid (1 equiv) in dry DMF (4 M) was added PyBOP (1 equiv) and compound **26** (1 equiv). The mixture was stirred for 5 min at room temperature before addition of Hünig's base (5 equiv). The resulting mixture was stirred at room temperature for 2 h, reduced in vacuo, and subsequently purified by flash chromatography on a C18 column (prepacked columns, 25−40 μm, Merck) using a linear gradient (95% C to 100% D in 30 min, flow rate of 15 mL·min^{-1}) of solvent D (100% CH_3CN) in solvent C (100% H_2O).

5-(*N*-(5-((1-(4-([1,1′-Biphenyl]-2-ylcarboxamido)benzoyl)-2,3,4,5-tetrahydro-1*H*-benzo[*b*]azepin-5-yl)amino)-5-oxopentyl)sulfamoyl)-2-(6-(diethylamino)-3-(diethyliminio)-3*H*-xanthen-9-yl)benzenesulfonate (28). Red powder (5 mg, 50%), mp 202−203 °C. ^{1}H NMR (400 MHz, $CDCl_3$): δ 8.65 (s, 1 H), 7.98 (d, J = 8.0 Hz, 1 H), 7.57 (d, J = 7.9 Hz, 1 H), 7.40 (d, J = 7.7 Hz, 1 H), 7.32 (d, J = 6.8 Hz, 4 H), 7.23−7.16 (m, 7 H), 7.11−7.04 (m, 5 H), 6.84 (t, J = 7.5 Hz, 1 H), 6.76 (td, J = 9.5, 2.3 Hz, 2 H), 6.63 (sl, 2 H), 6.46 (s, J = 7.5 Hz, 1 H), 5.19 (d, J = 10.4 Hz, 1 H), 4.46 (sl, 1 H), 3.53−3.46 (m, 8 H), 3.30−3.29 (m, 1 H), 2.95 (sl, 1 H), 2.27 (t, J = 7.6 Hz, 2 H), 1.99 (sl, 1 H), 1.88 (sl, 1 H), 1.75−1.66 (m, 2 H), 1.59−1.51 (m, 4 H), 1.35−1.30 (m, 4 H), 1.24−1.20 (m, 12 H). ^{13}C NMR (75 MHz, $CDCl_3$): δ 169.9, 158.9, 157.9, 155.7, 146.8, 145.8, 142.9, 140.6, 139.9, 138.7, 135.8, 133.6, 132.9, 130.5, 130.3, 129.5, 128.7, 128.6, 128.4, 127.8, 127.6, 127. 5, 126.8, 124.3, 118.7, 114.2, 113.8, 95.8, 54.4, 46.8, 45.9, 42.6, 42.6, 35.6, 31.2, 29.1, 22.9, 12.6. RP-HPLC purity: 95%; t_R = 15.54. HR-MS for $C_{62}H_{65}N_6O_9S_2$: calcd 1101.4249, found: 1101.4245.

5-((4-(3-((1-(4-([1,1′-Biphenyl]-2-ylcarboxamido)benzoyl)-2,3,4,5-tetrahydro-1*H*-benzo[*b*]azepin-5-yl)amino)-3-oxopropyl)piperazin-1-yl)sulfonyl)-2-(6-(diethylamino)-3-(diethyliminio)-3*H*-xanthen-9-yl)benzenesulfonate (29). Red powder (24 mg, 67%); mp 233−234 °C. ^{1}H NMR (400 MHz, CD_3OD): δ 8.61 (s, 1H), 8.02 (d, J = 8.1 Hz, 1H), 7.53−7.21 (m, 16H), 7.10−6.94 (m, 10H), 6.83−6.67 (m, 4H), 6.59 (d, J = 7.5 Hz, 1H), 5.30 (d, J = 10.0 Hz, 1H), 4.54 (sl, 1H), 3.65−3.54 (m, 8H), 3.27 (sl, 3H), 3.04 (sl, 1H), 2.87−2.28 (m, 7H), 2.05 (sl, 2H), 1.66 (sl, 2H), 1.30−1.26 (m, 12H). ^{13}C NMR (75 MHz, CD_3OD): δ 173.5, 171.2, 170.9, 159.1, 157.4, 156.9, 147.6, 141.7, 141.2, 139.9, 139.0, 137.4, 135.9, 133.6, 133.5, 132.3, 132.0, 131.2, 130.3, 129.8, 129.5, 129.3, 128.8, 128.6, 128.6, 128.4, 128.3, 125.6, 119.9, 115.1, 114.9, 96.9, 54.9, 53.0, 51.6, 47.2, 46.8, 34.0, 32.4, 26.3, 13.0. RP-HPLC purity: >95%; t_R = 14.20. HR-MS for $C_{64}H_{68}N_7O_9S_2$: calcd: 1142.4514, found: 1142.4495.

5-(*N*-(2-(2-(2-(3-((1-(4-([1,1′-Biphenyl]-2-ylcarboxamido)benzoyl)-2,3,4,5-tetrahydro-1*H*-benzo[*b*]azepin-5-yl)amino)-3-oxopropoxy)ethoxy)ethoxy)ethyl)sulfamoyl)-2-(6-(diethylamino)-3-(diethyliminio)-3*H*-xanthen-9-yl)benzenesulfonate (30). Red powder (15 mg, 40%); mp 182−183 °C. ^{1}H NMR (400 MHz, $CDCl_3$): δ 8.83 (s, 1 H), 8.01 (d, J = 7.9 Hz, 1H), 7.73 (d, J = 7.9 Hz, 1H), 7.46 (d, J = 7.6 Hz, 1H), 7.41−7.27 (m, 10H), 7.21−7.18 (m, 3H), 7.06 (t, J = 7.7 Hz, 2H), 6.85−6.73 (m, 4H), 6.64 (sl, 2H), 6.47 (d, J = 7.6 Hz, 1H), 5.18 (sl, 1H), 4.50 (sl, 1H), 3.85 (t, J = 6.2 Hz, 2H), 3.71−3.65 (m, 10H), 3.56−3.46 (m, 10H), 3.25 (sl, 2H), 2.92 (sl, 1H), 1.90 (sl, 2H), 1.63 (sl, 1H), 1.54 (sl, 1H), 1.27−1.24 (m, 12H). ^{13}C NMR (75 MHz, $CDCl_3$): δ 158.4, 158.0, 155.8, 142.7, 140.9, 139.9, 139.1, 133.8, 133.4, 130.8, 130.5, 130.2, 129.8, 129.5, 129.1, 128.8, 128.3, 128.2, 127.9, 127.9, 127.6, 127.4, 127.3, 125.1, 118.8, 114.5, 113.9, 95.9, 77.4, 70.5, 70.4, 70.4, 70.3, 69.9, 67.9, 50.9, 46.9, 46.1, 43.3, 36.8, 31.2, 25.6, 12.8. RP-HPLC purity: >95%; t_R = 15.54. HR-MS for $C_{66}H_{73}N_6O_{12}S_2$: calcd 1205.4722, found: 1205.4703.

***N*^{1}-(1-(4-([1,1′-Biphenyl]-2-ylcarboxamido)benzoyl)-2,3,4,5-tetrahydro-1*H*-benzo[b]azepin-5-yl)-*N*^{4}-(prop-2-yn-1-yl)-succinamide (39).** A solution of compound **26** (54 mg, 0.117 mmol) in DMF (0.6 mL) was slowly added to a solution of compound **31** (15 mg, 0.10 mmol) dissolved in DMF (0.6 mL) in the presence of PyBOP (61 mg, 0.12 mmol) and Hünig's base (51 μL, 0.29 mmol). Following 16 h stirring at room temperature, the mixture was concentrated in vacuo. The residue was dissolved in EtOAc (5 mL) and washed sequentially with a saturated solution of $NaHCO_3$ and brine. The organic layer was concentrated in vacuo and the residue purified by flash chromatography. Compound **39** was obtained as a clear oil (47 mg, 87%). ^{1}H NMR (400 MHz, CD_3OD): δ 7.50 (t, J = 7.6 Hz, 2H), 7.36−7.41 (m, 4H), 7.15−7.28 (m, 10H), 6.95 (t, J = 7.8 Hz, 1H), 5.24−5.27 (m, 1H), 3.93 (t, J = 2.2 Hz, 2H), 3.27 (m, 4H), 2.60−2.67 (m, 2H), 2.52−2.55 (m, 3H), 1.97−206 (m, 2H), 1.60−1.67 (m, 2H), 1.25 ppm (s, 1H). ^{13}C NMR (75 MHz, CD_3OD): δ 141.9, 141.9, 141.4, 141.4, 141.4, 141.4, 140.4, 137.8, 132.5, 131.4, 131.3, 130.3, 129.7, 129.6, 129.5, 129.5, 128.9, 128.6, 128.5, 128.4, 125.6, 120.1, 80.7, 72.3, 51.8, 48.0, 32.7, 31.9, 30.8, 29.6, 26.6. RP-HPLC purity: >95%; t_R = 14.18. ES-MS for $C_{37}H_{35}N_4O_4$: calcd 599.26, found 599.25.

Fluorescein Labeled Compound (40). To a solution of compound **39** (23 mg, 0.04 mmol) and compound **37** (26 mg, 0.04 mmol) in a DMF/H_2O (9/1, v/v, 0.8 mL) mixture was added 10% of sodium ascorbate (1 mg, 0.005 mmol), dissolved in the minimum of water, 10% of TBTA (2 mg, 0.005 mmol) dissolved in the minimum of DMF, and finally $CuSO_4·5H_2O$ (0.6 mg, 0.004 mmol). After 5 h at room temperature, the mixture was concentrated in vacuo to a residue that was purified by RP-HPLC on a C18 Symmetry Shield column (19 mm × 300 mm) following a linear gradient from 20% to 70% of solvent B in solvent A in 40 min (10 mL·min^{-1}, detection at 220 and 254 nm). Following a freeze-drying step, compound **40** was obtained as an orange-colored powder (12 mg, 26%); mp 154−155 °C; t_R = 14.48. HRMS for $C_{66}H_{64}N_9O_{12}S$: calcd 1206.4395, found 1206.4412.

General Procedure for the Preparation of Compounds 41, 42, and 43 by Solution-Phase "Click" Chemistry. To a solution of

dx.doi.org/10.1021/jm3006146 | J. Med. Chem. XXXX, XXX, XXX−XXX

benzazepine−acetylene (1 equiv) and fluorescent azido spacer (1.2 equiv) in a DMF/H_2O (9/1, v/v) mixture was added sodium ascorbate (0.1 equiv), presolubilized in the minimum of water and $CuSO_4 \cdot 5H_2O$ (0.1 equiv) also presolubilized in the minimum of water. Following 2 h stirring at room temperature, the mixture was concentrated in vacuo and the residue purified by RP-HPLC on a C18 Symmetry Shield column (19 mm × 300 mm) following a linear gradient from 5% to 60% of solvent B in solvent A in 30 min (10 mL·min^{-1}, detection at 220 and 254 nm).

*N^1-(1-(4-([1,1′-Biphenyl]-2-ylcarboxamido)benzoyl)-2,3,4,5-tetrahydro-1H-benzo[b]azepin-5-yl)-N^4-((1-(3-aminopropyl)-1H-1,2,3-triazol-4-yl)methyl)succinamide (**41**).* White powder (10 mg, 29%); mp 153−155 °C. ^{1}H NMR (400 MHz, CD_3OD): δ 7.90 (s, 1 H), 7.55 (t, J = 7.8 Hz, 2 H), 7.46 (d, J = 7.8 Hz, 2 H), 7.40 (d, J = 7.8 Hz, 2 H), 7.33−7.23 (m, 8 H), 7.19 (t, J = 7.3 Hz, 1 H), 7.01 (t, J = 7.3 Hz, 1 H), 6.66 (d, J = 7.3 Hz, 2 H), 5.30 (dd, J = 11.3, 3.5 Hz, 1 H), 5.10−4.94 (m, 2 H), 4.60−4.33 (m, 6 H), 2.74−2.71 (m, 2 H), 2.62−2.58 (m, 2 H), 2.14−2.00 (m, 2 H), 1.72−1.67 (m, 2 H). ^{13}C NMR (75 MHz, CD_3OD): δ 174.2, 174.1, 171.6, 171.5, 141.9, 141.6, 141.5, 141.4, 140.7, 137.8, 132.7, 131.6, 131.5, 130.5, 129.8, 129.7, 129.6, 129.1, 128.9, 128.7, 128.6, 51.9, 48.2, 40.3, 36.1, 32.7, 32.0, 31.8, 26.5. RP-HPLC purity: 95%; t_R = 8.08. HRMS for $C_{39}H_{40}N_8O_4$: calcd 684.3173, found 685.3181.

*N^1-(1-(4-([1,1′-Biphenyl]-2-ylcarboxamido)benzoyl)-2,3,4,5-tetrahydro-1H-benzo[b]azepin-5-yl)-N^4-((1-(2-(2-(2-(2-aminoethoxy)-ethoxy)ethoxy)ethyl)-1H-1,2,3-triazol-4-yl)methyl)succinamide (**42**).* White powder (15 mg, 44%), mp 95−97 °C. ^{1}H NMR (400 MHz, $CDCl_3$): δ 10.26 (s, 1 H), 8.55 (d, J = 7.6 Hz, 1 H), 8.37 (t, J = 5.6 Hz, 1 H), 7.75 (sl, 2 H), 7.57−7.52 (m, 2 H), 7.48−7.43 (m, 2 H), 7.38−7.21 (m, 9 H), 7.16 (t, J = 7.6 Hz, 1 H), 6.98 (t, J = 6.4 Hz, 1 H), 6.63 (d, J = 7.4 Hz, 1 H), 5.14 (sl, 1 H), 4.43 (t, J = 5.1 Hz, 2 H), 4.30 (t, J = 6.0 Hz, 1 H), 3.76 (t, J = 5.3 Hz, 2 H), 3.5 (sl, 1 H), 2.96 (q, J = 10.9, 5.4 Hz, 2 H), 2.44 (q, J = 13.8, 7.2 Hz, 2 H), 1.99 (sl, 1 H), 1.88 (sl, 1 H), 1.57 (sl, 2 H). ^{13}C NMR (75 MHz, CD_3OD): δ 174.8, 174.1, 171.5, 171.4, 142.0, 141.6, 141.5, 140.6, 132.6,131.5, 131.4, 130.5, 129.8, 129.7, 129.6, 129.1, 128.9, 128.7, 128.6, 125.7, 120.7, 71.6, 71.4, 71.3, 70.4, 67.9, 51.9, 51.4, 48.1, 40.8, 35.9, 32.7, 32.1, 32.0, 26.6. RP-HPLC purity: >95%; t_R = 8.22. HRMS for $C_{45}H_{53}N_8O_7$: calcd 817.4037, found 817.4032.

*N^1-(1-(4-([1,1′-Biphenyl]-2-ylcarboxamido)benzoyl)-2,3,4,5-tetrahydro-1H-benzo[b]azepin-5-yl)-N^4-((1-(20-amino-3,6,9,12,15,18-hexaoxaicosyl)-1H-1,2,3-triazol-4-yl)methyl)succinamide (**43**).* Syrup solid (12 mg, 33%). ^{1}H NMR (400 MHz, CD_3OD): δ 7.89 (s, 1 H), 7.55 (t, J = 7.8 Hz, 2 H), 7.46 (d, J = 7.8 Hz, 2 H), 7.41 (d, J = 7.8 Hz, 2 H), 7.33−7.24 (m, 8 H), 7.20 (t, J = 7.3 Hz, 1 H), 7.01 (t, J = 7.4 Hz, 1 H), 6.66 (d, J = 7.4 Hz, 2 H), 5.31 (dd, J = 11.4, 3.5 Hz, 1 H), 4.59−4.38 (m, 6 H), 3.77 (t, J = 4.8 Hz, 2 H), 3.71−3.54 (m, 22 H), 3.09−3.07 (m, 2 H), 2.74−2.70 (m, 2 H), 2.61−2.57 (m, 2 H), 2.15−2.00 (m, 2 H), 1.74−1.65 (m, 2 H). ^{13}C NMR (75 MHz, CD_3OD): δ 174.8, 174.1, 171.5, 171.3, 142.0, 141.6, 141.5, 140.7, 137.9, 132.7, 131.5, 131.4, 130.5, 129.8, 129.7, 129.6, 129.1, 128.9, 128.7, 128.6, 125.7, 120.3, 71.6, 71.5, 71.4, 71.3, 71.2, 70.9, 70.4, 68.0, 51.9, 51.4, 48.1, 40.6, 36.0, 32.7, 32.1, 32.0, 26.6. RP-HPLC purity: >95%; t_R = 8.34. HR-MS for $C_{51}H_{64}N_8O_{10}$: calcd 948.4745, found 948.4749.

General Procedure for the Solution-Phase Coupling of DY647 and Lumi4-Tb Dyes onto Compounds (41−43). A solution of DY647-NHS or Lumi4-Tb-NHS (1 equiv) in anhydrous dimethylsulfoxide was added to a solution of amino-benzazepine (1 equiv) presolubilized in anhydrous dimethylsulfoxide. Following addition of Hünig's base (7 equiv), the mixture was stirred at room temperature under argon atmosphere for 1 h. The completion of the reaction was monitored by analytical RP-HPLC. The mixture was diluted in an acetonitrile solution containing 0.2% of trifluoroacetic acid for DY647 probes or triethylammonium acetate buffer (25 mM, pH 7) for Lumi4-Tb probes. The expected labeled compounds were isolated by RP-HPLC on a C18 column either using a linear gradient of solvent C (100% acetonitrile) in solvent A (100% H_2O, 0.1% TFA, v/v) for DY647 probes and a linear gradient of solvent C in solvent E (triethylammonium acetate buffer, 25 mM, pH 7) for Lumi4-Tb probes. Fractions containing the products of interest were pooled, concentrated, and further checked for purity by analytical RP-HPLC and HRMS as indicated.

DY647 Labeled Compound 44. Blue powder (405 nmol, 40%). UV (water): λ_{max} 650 nm. RP-HPLC purity: >95%; t_R = 9.85. HR-MS for $C_{71}H_{76}N_{10}O_{11}S_2$: calcd 1308.5136, found 1308.5131.

DY647 Labeled Compound 45. Blue powder (1480 nmol, 74%). UV (water): λ_{max} 650 nm. RP-HPLC purity: >95%; t_R = 9.90. HR-MS for $C_{77}H_{88}N_{10}O_{14}S_2$: calcd 1440.5922, found 1441.5927.

DY647 Labeled Compound 46. Blue powder (890 nmol, 89%). UV (water): λ_{max} 650 nm. RP-HPLC purity: >95%; t_R = 9.97. HR-MS for $C_{83}H_{100}N_{10}O_{17}S_2$: calcd 1572.6708, found 1572.6712.

Lumi4-Tb Labeled Compound 47. White powder (165 nmol, 16%). UV (water): λ_{max} 339 nm. RP-HPLC purity: >95%; t_R = 10.10. HR-MS for $C_{103}H_{120}N_{21}O_{18}Tb$: calcd 2097.8373, found 2098.8350.

Lumi4-Tb Labeled Compound 48. White powder (180 nmol, 45%). UV (water): λ_{max} 339 nm. RP-HPLC purity: >95%; t_R = 10.18. HR-MS for $C_{109}H_{132}N_{21}O_{21}Tb$: calcd 2229.9160, found 2230.9189.

Lumi4-Tb Labeled Compound 49. White powder (380 nmol, 38%). UV (water): λ_{max} 337 nm. RP-HPLC purity: >95%; t_R = 10.31. HR-MS for $C_{115}H_{144}N_{21}O_{24}Tb$: calcd 2361.9946, found 2362.9960.

Radioligand Binding Assays. Binding assays were performed at 30 °C using [^{3}H]-AVP as radioligand and 5 μg of CHO cell membrane proteins. Briefly, membranes prepared from CHO cells stably expressing either the human V_2R, $V_{1a}R$, $V_{1b}R$, or the human OTR, were incubated in 50 mM Tris-HCl pH 7.4, 5 mM $MgCl_2$ supplemented with 1 mg/mL BSA (binding buffer) and with radiolabeled and displacing ligands for 30 min. The affinitiy (K_d) for [^{3}H]-AVP to the different human receptor subtypes has already been described earlier.[39] Affinities (K_i) for other compounds were determined by competition experiments using [^{3}H]-AVP (1−2 nM) and varying concentrations of the unlabeled ligands from 100 pM to 100 μM. The nonspecific binding was determined by adding unlabeled AVP (10 μM). Bound and free radioactivity were separated by filtration over Whatman GF/C filters presoaked in a 10 mg·mL^{-1} BSA solution for 3−4 h. The ligand binding data were analyzed by nonlinear least-squares regression using the computer program Ligand. All assays were performed in triplicate on at least three independent batches of cell membranes.

cAMP Accumulation Assays. Accumulation of cAMP was quantified using the cAMP dynamic 2 Kit (Cisbio Bioassays, Codolet, France) based on a homogeneous TR-FRET technology (HTRF).[13] Briefly, 5 × 10^3 CHO cells stably expressing the human V_2R were seeded into each well of a 96-well plate pretreated with polyornithine. Then 24 h later, cells were incubated 30 min at 37 °C in the cAMP buffer with or without increasing compound (AVP or fluorescent ligands) concentrations (10^{-12} to 10^{-5} M) in the presence of the phosphodiesterase inhibitor RO 201724 0.1 mM (Sigma). The activity of antagonists was measured in the presence of 1 nM AVP in order to detect a dose-dependent AVP-induced cAMP inhibition. Cells were then lyzed, and cAMP levels were determined.[17]

Fluorescent Ligand-Binding Assays. These assays were performed as described in Zwier et al,.[48] Briefly, HEK 293T cells were cultivated in DMEM medium supplemented with 10% fetal calf serum (FCS) and 1% penicillin/streptomycin antibiotics. As described in Cottet et al,[49] confluent cells were dissociated and electroporated with plasmid DNA coding for the V2 receptor fused to the SNAP-tag suicide enzyme. Transfected cells were then plated in black 96-well plates previously coated with polyornithine (diluted at 0.1 mg·mL^{-1} in sterile water, incubated 30 min at 37 °C, washed with sterile PBS). Plates were incubated in supplemented DMEM medium for 48 h at 37 °C, 95% O_2, and 5% CO_2. Expressed receptors fused to SNAP-tag were then labeled with fluorescent substrates, either with a donor (SNAP-Lumi4-Tb) or an acceptor (SNAP-RED) at respectively 100 or 300 nM in 100 μL of Tag-lite labeling medium, for 1 h at 37 °C. Cells were then washed 3 times in Tag-lite medium and then incubated with the fluorescent ligands. For saturation assays, increasing concentrations of fluorescent ligands were diluted in 100 μL of Tag-lite medium. For competition assays, a fixed concentration of fluorescent ligand (typically 20 nM) was mixed with an increasing concentration of

dx.doi.org/10.1021/jm3006146 | J. Med. Chem. XXXX, XXX, XXX−XXX

cold competitor ligand (in this case AVP) in Tag-lite medium. After overnight incubation at 4 °C (to prevent any internalization phenomenon), plates were read in an HTRF-compatible multiwell plate reader with a classic HTRF protocol (excitation at 340 nM, donor emission measured at 620 nm and acceptor emission at 665 nm, 50 μs delay, 500 μs integration).

Receptor Dimerization Assay. Cos7 cells expressing either SNAP-V1a or SNAP-V2 or both receptors were seeded in 96-well plate format at a density of 50000 cells/well. Cells were incubated in the presence of a mix of fluorescent ligands (one donor and one acceptor fluorescent ligand) at a concentration close to their K_d. Time-resolved FRET signal was read after an overnight incubation at 4 °C. Nonspecific time-resolved FRET was determined by incubating Mock cells in the presence of fluorescent ligands. Time-resolved FRET is expressed as % ΔF equal to $(R_{sample} - R_{negative})/R_{negative}$), where R is the ratio of fluorescence intensities measured at 665 and 620 nm when the sample is excitated at 335 nm. $R_{negative}$ is a nonspecific FRET ratio determined on Mock cells. Expression of each receptor is estimated by using the Tag-lite labeling strategy. Cells expressing tagged receptors were incubated in the presence of 100 nM of fluorescent benzylguanine subtrates (SNAP-Lumi4-Tb) for 1 h at room temperature and rinsed twice with PBS, and fluorescent intensity of each samples excited at 335 nm was measured at 620 nm.

Molecular Modeling. Human M1R (UNIPROT: ACM1_human) was modeled by homology to the rat muscarinic M3 receptor (PDB: 4daj, chain A) using MOE 2011 (Chemical Computing Group Inc., Montreal, Canada). The three-dimensional structure of Bo(10)Pz was generated using Corina 3.1 (Molecular Network GmbH, Erlangen, Germany) and then docked into the transmembrane cavity of M1R using Surflex v2.6 (BioPharmics LCC, San Mateo, CA, USA). Detailed parameters for homology modeling and docking are provided in the Supporting Information S-5.

The 3D-structure of the phenyl benzazepine moiety of compound **27** was modeled from the crystal coordinates of MUPTAS entry of the Cambridge Chemical Databank. The structure of compound **27** was completed using MOE 2011 and then energy minimized (default settings) in the MMFF94X force field. A total of 17 low-energy conformations were obtained for compound **27** using the Low-ModeMD search of MOE 2011 (default settings, except the value of 5 kcal/mol specified for Energy Window, and the root-mean-square deviation of coordinates of the phenyl benzazepine moiety of compound **27** from the input structure lower than 0.6 Å).

■ ASSOCIATED CONTENT

Supporting Information

Procedure for the preparation of *para*-LRB sulfonyl chloride; experimental details and characterizations for compounds **12**–**15**, **17**, **19**, **31**, **33**–**35**, and **37**. Modeling and docking parameters, EGFP-V_2R expression; absorption and emission spectra of Lumi4-Tb and DY647, sequence alignment for homology modeling of M1R and V_2R, three-dimensional models of M1R and V_2R bound to fluorescent ligands, and functional activity of EGFP-V_2R in presence of AVP. This material is available free of charge via the Internet at http://pubs.acs.org.

■ AUTHOR INFORMATION

Corresponding Author

*Phone: +33 368 85 42 36. Fax: +33 368 85 43 10. E-mail: dominique.bonnet@unistra.fr.

Notes

The authors declare no competing financial interest.

■ ACKNOWLEDGMENTS

This work was supported by the Centre National de la Recherche Scientifique, the Université de Strasbourg, the Région Alsace (Stephanie Loison fellowship), the Institut National de la Santé et de la Recherche Médicale and the Université Montpellier I and II. We are grateful to Christel Valencia and Dr. Pascal Villa (PCBIS platform, UMS 3286, ESBS, Illkirch, France) for EGPF-V_2R expression. We thank Pascale Buisine and Patrick Wehrung for ES-MS analyses. The skillful technical assistance of Stéphanie Riché was greatly appreciated.

■ ABBREVIATIONS USED

AVP, arginine-vasopressin; EGFP, enhanced green fluorescent protein; FRET, fluorescence resonance energy transfer; GPCRs, G protein-coupled receptors; HBTU, *N*-[(1*H*benzotriazol-1-yl)(dimethylamino)methylene]-*N*-methylmethanaminium hexafluorophosphate *N*-oxide; HOBt, *N*-hydroxybenzotriazole; HRMS, high resolution mass spectrometry; TR-FRET, time-resolved FRET; HTS, high-throughput screening; M1R, human muscarinic M1 receptor; LRB, Lissamine Rhodamine B; NHS, *N*-hydroxysuccinimide; OTR, oxytocin receptor; PyBOP, benzotriazole-1-yl-oxytrispyrrolidinophosphonium hexafluorophosphate; SPOrT, solid-phase organic tagging; TBTA, tris[(1-benzyl-1*H*-1,2,3-triazol-4-yl)methyl]amine; TMSOTf, trimethylsilyl trifluoromethanesulfonate; TM, transmembrane domain; V_2R, arginine-vasopressin V_2 receptor

■ REFERENCES

(1) Thomsen, W.; Frazer, J.; Unett, D. Functional assays for screening GPCR targets. *Curr. Opin. Biotechnol.* **2005**, *16* (6), 655–665.

(2) Drews, J. Drug discovery: a historical perspective. *Science* **2000**, *287* (5460), 1960–1964.

(3) Ma, P.; Zemmel, R. Value of novelty? *Nature Rev. Drug Discovery* **2002**, *1* (8), 571–572.

(4) Hovius, R.; Vallotton, P.; Wohland, T.; Vogel, H. Fluorescence techniques: shedding light on ligand–receptor interactions. *Trends Pharmacol. Sci.* **2000**, *21* (7), 266–273.

(5) Owicki, J. C. Fluorescence polarization and anisotropy in high throughput screening: perspectives and primer. *J. Biomol. Screening* **2000**, *5* (5), 297–306.

(6) Allen, M.; Reeves, J.; Mellor, G. High throughput fluorescence polarization: a homogeneous alternative to radioligand binding for cell surface receptors. *J. Biomol. Screening* **2000**, *5* (2), 63–69.

(7) Albizu, L.; Teppaz, G.; Seyer, R.; Bazin, H.; Ansanay, H.; Manning, M.; Mouillac, B.; Durroux, T. Toward efficient drug screening by homogeneous assays based on the development of new fluorescent vasopressin and oxytocin receptor ligands. *J. Med. Chem.* **2007**, *50* (20), 4976–4985.

(8) Tahtaoui, C.; Parrot, I.; Klotz, P.; Guillier, F.; Galzi, J. L.; Hibert, M.; Ilien, B. Fluorescent pirenzepine derivatives as potential bitopic ligands of the human M1 muscarinic receptor. *J. Med. Chem.* **2004**, *47* (17), 4300–4315.

(9) Szollosi, J.; Damjanovich, S.; Matyus, L. Application of fluorescence resonance energy transfer in the clinical laboratory: routine and research. *Cytometry* **1998**, *34* (4), 159–179.

(10) Daval, S. B.; Valant, C.; Bonnet, D.; Kellenberger, E.; Hibert, M.; Galzi, J. L.; Ilien, B. Fluorescent Derivatives of AC-42 To Probe Bitopic Orthosteric/Allosteric Binding Mechanisms on Muscarinic M1 Receptors. *J. Med. Chem.* **2012**, *55* (5), 2125–2143.

(11) Marie, J.; Leyris, J. P.; Roux, T.; Trinquet, E.; Verdie, P.; Fehrentz, J. A.; Oueslati, N.; Douzon, S.; Bourrier, E.; Lamarque, L.; Gagne, D.; Galleyrand, J. C.; M'kadmi, C.; Martinez, J.; Mary, S.; Baneres, J. L. Homogeneous time-resolved fluorescence-based assay to screen for ligands targeting the growth hormone secretagogue receptor type 1a. *Anal. Biochem.* **2011**, *408* (2), 253–262.

(12) Degorce, F.; Card, A.; Soh, S.; Trinquet, E.; Knapik, G. P.; Xie, B. HTRF: A technology Tailored for Drug Discovery—A review of

Theoretical Aspects and Recent Applications. *Curr. Chem. Genomics* **2009**, *3*, 22−32.
(13) Pin, J. P.; Maurel, D.; Comps-Agrar, L.; Brock, C.; Rives, M. L.; Bourrier, E.; Ayoub, M. A.; Bazin, H.; Tinel, N.; Durroux, T.; Prezeau, L.; Trinquet, E. Cell-surface protein−protein interaction analysis with time-resolved FRET and snap-tag technologies: application to GPCR oligomerization. *Nature Methods* **2008**, *5* (6), 561−567.
(14) Albizu, L.; Cottet, M.; Kralikova, M.; Stoev, S.; Seyer, R.; Brabet, I.; Roux, T.; Bazin, H.; Bourrier, E.; Lamarque, L.; Breton, C.; Rives, M. L.; Newman, A.; Javitch, J.; Trinquet, E.; Manning, M.; Pin, J. P.; Mouillac, B.; Durroux, T. Time-resolved FRET between GPCR ligands reveals oligomers in native tissues. *Nature Chem. Biol.* **2010**, *6* (8), 587−594.
(15) Middleton, R. J.; Kellam, B. Fluorophore-tagged GPCR ligands. *Curr. Opin. Chem. Biol.* **2005**, *9* (5), 517−525.
(16) Robertson, G. L. Vaptans for the treatment of hyponatremia. *Nature Rev. Endocrinol.* **2011**, *7* (3), 151−161.
(17) Arai, Y.; Fujimori, A.; Sudoh, K.; Sasamata, M. Vasopressin receptor antagonists: potential indications and clinical results. *Curr. Opin. Pharmacol.* **2007**, *7* (2), 124−129.
(18) Jean-Alphonse, F.; Perkovska, S.; Frantz, M. C.; Durroux, T.; Mejean, C.; Morin, D.; Loison, S.; Bonnet, D.; Hibert, M.; Mouillac, B.; Mendre, C. Biased Agonist Pharmacochaperones of the AVP V2 Receptor May Treat Congenital Nephrogenic Diabetes Insipidus. *J. Am. Soc. Nephrol.* **2009**, *20* (10), 2190−2203.
(19) Manning, M.; Misicka, A.; Olma, A.; Bankowski, K.; Stoev, S.; Chini, B.; Durroux, T.; Mouillac, B.; Corbani, M.; Guillon, G. Oxytocin and Vasopressin Agonists and Antagonists as Research Tools and Potential Therapeutics. *J. Neuroendocrinol.* **2012**, *24* (4), 609−628.
(20) Mouillac, B.; Manning, M.; Durroux, T. Fluorescent agonists and antagonists for vasopressin/oxytocin G protein-coupled receptors: usefulness in ligand screening assays and receptor studies. *Mini-Rev. Med. Chem.* **2008**, *8* (10), 996−1005.
(21) Durroux, T.; Peter, M.; Turcatti, G.; Chollet, A.; Balestre, M. N.; Barberis, C.; Seyer, R. Fluorescent pseudo-peptide linear vasopressin antagonists: design, synthesis, and applications. *J. Med. Chem.* **1999**, *42* (7), 1312−1319.
(22) Bonnet, D.; Riche, S.; Loison, S.; Dagher, R.; Frantz, M. C.; Boudier, L.; Rahmeh, R.; Mouillac, B.; Haiech, J.; Hibert, M. Solid-phase organic tagging resins for labeling biomolecules by 1,3-dipolar cycloaddition: application to the synthesis of a fluorescent non-peptidic vasopressin receptor ligand. *Chem.—Eur. J.* **2008**, *14* (20), 6247−6254.
(23) Ogawa, H.; Yamashita, H.; Kondo, K.; Yamamura, Y.; Miyamoto, H.; Kan, K.; Kitano, K.; Tanaka, M.; Nakaya, K.; Nakamura, S.; Mori, T.; Tominaga, M.; Yabuuchi, Y. Orally active, nonpeptide vasopressin V2 receptor antagonists: a novel series of 1-[4-(benzoylamino)benzoyl]-2,3,4,5-tetrahydro-1*H*-benzazepines and related compounds. *J. Med. Chem.* **1996**, *39* (18), 3547−3555.
(24) Matsuhisa, A.; Tanaka, A.; Kikuchi, K.; Shimada, Y.; Yatsu, T.; Yanagisawa, I. Nonpeptide arginine vasopressin antagonists for both V1A and V2 receptors: synthesis and pharmacological properties of 2-phenyl-4′-[(2,3,4,5-tetrahydro-1*H*-1-benzazepin-1-yl)carbonyl]-benzanilide derivatives. *Chem. Pharm. Bull. (Tokyo)* **1997**, *45* (11), 1870−1874.
(25) Rzepecki, P.; Geib, N.; Peifer, M.; Biesemeier, F.; Schrader, T. Synthesis and binding studies of Alzheimer ligands on solid support. *J. Org. Chem.* **2007**, *72* (10), 3614−3624.
(26) Wermuth, C. G. Preparation of Water-Soluble Compounds by Covalent Attachment of Solubilizing Moieties. In *The Practice of Medicinal Chemistry*, 2nd ed.; Wermuth, C. G., Eds.; Elsevier Academic Press: New York, 2003; pp 626−627.
(27) Jia, J.; Wang, K.; Shi, W.; Chen, S. M.; Li, X. H.; Ma, H. M. Rhodamine B Piperazinoacetohydrazine: A Water-Soluble Spectroscopic Reagent for Pyruvic Acid Labeling. *Chem.—Eur. J.* **2010**, *16* (22), 6638−6643.
(28) Bai, M.; Wyatt, S. K.; Han, Z.; Papadopoulos, V.; Bornhop, D. J. A novel conjugable translocator protein ligand labeled with a fluorescence dye for in vitro imaging. *Bioconjuate Chem.* **2007**, *18* (4), 1118−1122.
(29) Glunde, K.; Foss, C. A.; Takagi, T.; Wildes, F.; Bhujwalla, Z. M. Synthesis of 6′-*O*-lissamine-rhodamine B-glucosamine as a novel probe for fluorescence imaging of lysosomes in breast tumors. *Bioconjuate Chem.* **2005**, *16* (4), 843−851.
(30) Bonnet, D.; Ilien, B.; Galzi, J. L.; Riche, S.; Antheaune, C.; Hibert, M. A rapid and versatile method to label receptor ligands using "click" chemistry: Validation with the muscarinic M1 antagonist pirenzepine. *Bioconjuate Chem.* **2006**, *17* (6), 1618−1623.
(31) Xu, J. D.; Corneillie, T. M.; Moore, E. G.; Law, G. L.; Butlin, N. G.; Raymond, K. N. Octadentate Cages of Tb(III) 2-Hydroxyisophthalamides: A New Standard for Luminescent Lanthanide Labels. *J. Am. Chem. Soc.* **2011**, *133* (49), 19900−19910.
(32) Ghose, S.; Trinquet, E.; Laget, M.; Bazin, H.; Mathis, G. Rare earth cryptates for the investigation of molecular interactions in vitro and in living cells. *J. Alloys Compd.* **2008**, *451* (1−2), 35−37.
(33) Boeglin, D.; Bonnet, D.; Hibert, M. Solid-phase preparation of a pilot library derived from the 2,3,4,5-tetrahydro-1*H*-benzo[*b*]azepin-5-amine scaffold. *J. Comb. Chem.* **2007**, *9* (3), 487−500.
(34) Coste, J.; Le-Nguyen, D.; Castro, B. PyBOP: a new peptide coupling reagent devoid of toxic by-product. *Tetrahedron Lett.* **1990**, *31* (2), 205−208.
(35) Zhang, A. J.; Russell, D. H.; Zhu, J.; Burgess, K. A method for removal of N-BOC protecting groups from substrates on TFA-sensitive resins. *Tetrahedron Lett.* **1998**, *39*, 7439−7442.
(36) Corrie, J. E. T.; Davis, C. T.; Eccleston, J. F. Chemistry of sulforhodamine−amine conjugates. *Bioconjugate Chem.* **2001**, *12* (2), 186−194.
(37) Yang, H.; Vasudevan, S.; Oriakhi, C. O.; Shields, J.; Carter, R. G. Scalable synthesis of lissamine rhodamine B sulfonyl chloride and incorporation of xanthene derivatives onto polymer supports. *Synthesis (Stuttgart)* **2008**, No. 6, 957−961.
(38) Castro, B.; Dormoy, J. R.; Evin, G.; Selve, C. Reactions of Peptide Bond 0.4. Benzotriazonyl-*N*-Oxytridimelthylamino Phosphonium Hexafluorophosphate (BOP). *Tetrahedron Lett.* **1975**, No. 14, 1219−1222.
(39) Breton, C.; Chellil, H.; Kabbaj-Benmansour, M.; Carnazzi, E.; Seyer, R.; Phalipou, S.; Morin, D.; Durroux, T.; Zingg, H.; Barberis, C.; Mouillac, B. Direct identification of human oxytocin receptor-binding domains using a photoactivatable cyclic peptide antagonist: comparison with the human V1a vasopressin receptor. *J. Biol. Chem.* **2001**, *276* (29), 26931−26941.
(40) Jacobson, K. A. Functionalized Congener Approach to the Design of Ligands for G Protein-Coupled Receptors (GPCRs). *Bioconjugate Chem.* **2009**, *20* (10), 1816−1835.
(41) Karton, Y.; Baumgold, J.; Handen, J. S.; Jacobson, K. A. Molecular Probes for Muscarinic Receptors—Derivatives of the M1-Antagonist Telenzepine. *Bioconjugate Chem.* **1992**, *3* (3), 234−240.
(42) Kruse, A. C.; Hu, J. X.; Pan, A. C.; Arlow, D. H.; Rosenbaum, D. M.; Rosemond, E.; Green, H. F.; Liu, T.; Chae, P. S.; Dror, R. O.; Shaw, D. E.; Weis, W. I.; Wess, J.; Kobilka, B. K. Structure and dynamics of the M3 muscarinic acetylcholine receptor. *Nature* **2012**, *482* (7386), 552−556.
(43) Wu, B. L.; Chien, E. Y. T.; Mol, C. D.; Fenalti, G.; Liu, W.; Katritch, V.; Abagyan, R.; Brooun, A.; Wells, P.; Bi, F. C.; Hamel, D. J.; Kuhn, P.; Handel, T. M.; Cherezov, V.; Stevens, R. C. Structures of the CXCR4 Chemokine GPCR with Small-Molecule and Cyclic Peptide Antagonists. *Science* **2010**, *330* (6007), 1066−1071.
(44) Manglik, A.; Kruse, A. C.; Kobilka, T. S.; Thian, F. S.; Mathiesen, J. M.; Sunahara, R. K.; Pardo, L.; Weis, W. I.; Kobilka, B. K.; Granier, S. Crystal structure of the mu-opioid receptor bound to a morphinan antagonist. *Nature* **2012**, *485* (7398), 321−326.
(45) Ilien, B.; Franchet, C.; Bernard, P.; Morisset, S.; Weill, C. O.; Bourguignon, J. J.; Hibert, M.; Galzi, J. L. Fluorescence resonance energy transfer to probe human M1 muscarinic receptor structure and drug binding properties. *J. Neurochem.* **2003**, *85* (3), 768−778.

(46) Bazin, H.; Trinquet, E.; Mathis, G. Time resolved amplification of cryptate emission: a versatile technology to trace biomolecular interactions. *J. Biotechnol.* **2002**, *82* (3), 233−250.
(47) Keppler, A.; Gendreizig, S.; Gronemeyer, T.; Pick, H.; Vogel, H.; Johnsson, K. A general method for the covalent labeling of fusion proteins with small molecules in vivo. *Nature Biotechnol.* **2003**, *21* (1), 86−89.
(48) Zwier, J. M.; Roux, T.; Cottet, M.; Durroux, T.; Douzon, S.; Bdioui, S.; Gregor, N.; Bourrier, E.; Oueslati, N.; Nicolas, L.; Tinel, N.; Boisseau, C.; Yverneau, P.; Charrier-Savournin, F.; Fink, M.; Trinquet, E. A Fluorescent Ligand-Binding Alternative Using Tag-lite (R) Technology. *J. Biomol. Screening* **2010**, *15* (10), 1248−1259.
(49) Cottet, M; A., L.; Comps-Agrar, L; Trinquet, E; Pin, J. P.; Mouillac, B; Durroux, T. Time resolved FRET strategy with fluorescent ligands to analyze receptor interactions in native tissues: application to GPCR oligomerization. *Methods Mol. Biol.* **2011**, *746*, 373−387.

dx.doi.org/10.1021/jm3006146 | *J. Med. Chem.* XXXX, XXX, XXX−XXX